FINAL TECHNICAL REPORT

U. S. Geological Survey
National Earthquake Hazards Reduction Program
Award Number G15AP00025

Collaborative Research with Fugro Consultants, Inc. and the USGS: Pilot Study: Constraining the Presence and Location of the Piedmont Thrust Splay, Oakland, CA

Recipient:

Fugro Consultants, Inc.
1777 Botelho Drive, Suite 262
Walnut Creek, CA 94596

Principal Investigators:

David Trench, InfraTerra
220 4th St, Suite 102
Oakland, CA 94607
email: dtrench@infraterra.com; phone: (541) 740-8922

Rufus Catchings, U.S. Geological Survey
345 Middlefield Road M.S. 977
Menlo Park, CA 94025
email: catching@usgs.gov; phone: (650) 329-4749

and

Michael Buga, Fugro Consultants
1777 Botelho Drive, Suite 262
Walnut Creek, CA 94596
Email: m.buga@fugro.com; phone: (925) 949-7100

Term of Award:

January 2015 to December 2015

Research supported by the U.S. Geological Survey (USGS), Department of the Interior, under USGS award number G15AP00025. The views and conclusions contained in this document are those of the authors and should not be interpreted as necessarily representing the official policies, either expressed or implied, of the U.S. Government.

Award G15AP00025

Pilot Study: Constraining the Piedmont Thrust Splay, Oakland, CA

David Trench[1], Rufus Catchings [2],
Michael Buga[3], Justin T. Pearce[1],
Mark Goldamn[2], Joanne Chan[2], Coyn. Criley[2]

[1]*InfraTerra, Inc* , [2]*United States Geological Survey*, [3]*Fugro Consultants, Inc.*

dtrench@infraterra.com, *catching@usgs.gov*, *m.buga@fugro.com*, *jpearce@infraterra.com*, *goldman@usgs.gov*, *jchan@usgs.gov*, *ccriley@usgs.gov*

ABSTRACT

This collaborative initial study investigated the Piedmont thrust, referred to herein as the Piedmont reverse fault (PRF), a potential splay of the Hayward fault in an area of anomalously high topography west of the Hayward fault in Piedmont and north Oakland, California. Various geologists have mapped faults in the low hills between the main trace of the Hayward fault and the western margin of the East Bay Hills (e.g., Radbruch-Hall, 1974; Graymer et al., 1995; Graymer, 2000; Dibblee and Minch, 2005). However, little to no direct geologic evidence exists to demonstrate the presence or absence of a tectonic fault; a critical uncertainty for seismic hazard in the East Bay, given that co-seismic (re)activation of the PRF during a major Hayward fault earthquake could create significant economic losses through permanent ground deformation. This Pilot study is designed to: (1) provide evidence for the physical presence or absence of a fault that is mapped as the boundary between the Cretaceous bedrock and Pleistocene alluvial fans, as shown on some published maps, and if present, (2) constrain the location of the fault (if present) in this urbanized setting. The problem was addressed through the integration of three lines of independent evidence: (1) geomorphic analysis of LiDAR data, (2) a focused seismic reflection and tomography survey, and (3) an exploratory borehole program, coupled with existing borehole data. The Pilot study was undertaken in and near Dimond Canyon Park in Oakland, California. Results support the presence of a PRF that generally coincides with a previously mapped trace and is found to be steeply dipping to the east and likely connects to the Hayward fault at depth in a positive flower structure. In addition, this study may have found evidence for more than one fault strand in the study area, possibly suggesting a complicated fault framework in the shallow subsurface.

TABLE OF CONTENTS

ABSTRACT i
1.0 INTRODUCTION 1
2.0 TECTONIC SETTING AND PREVIOUS WORK 3
3.0 DIMOND CANYON PARK INVESTIGATION SITE 4
4.0 APPROACH AND METHODOLOGY 5
4.1 Compilation and Review of existing data 5
4.2 Seismic Data Collection 5
4.3 Borehole Data Collection 6
5.0 ANALYSIS AND RESULTS 7
5.1 Fault Perpendicular LiDAR Profiles 7
5.2 High resolution P- and S-wave seismic data 8
5.3 Footwall and Hanging-wall Exploratory Borings 11
6.0 SUMMARY OF FINDINGS 15
7.0 SIGNIFICANCE OF RESULTS 16
8.0 ACKNOWLEDGEMENTS 18
9.0 REFERENCES 19
10.0 FIGURES 22

LIST OF FIGURES

Figure 1. Shaded Relief Map of High Topography West of the Hayward Fault
Figure 2. Geologic Map of the Study Region
Figure 3. Quaternary Geology of the Study Area Showing Data Collection Locations
Figure 4. Example P-wave shot gathers
Figure 5. Example S-wave shot gathers
Figure 6. Shaded Relief Map of Piedmont Reverse Fault Showing Topographic Profile Locations
Figure 7. Topographic profiles Across the Piedmont Reverse Fault

Figure 8. P-wave Refraction Tomography Velocity Model Cross-section, Un-interpreted (Top) and Interpreted (Bottom)
Figure 9. S-wave Refraction Tomography Velocity Model Cross-section, Un-interpreted (Top) and Interpreted (Bottom)
Figure 10. Vp/Vs ratio model Cross-section, Un-interpreted (Top) and Interpreted (Bottom)
Figure 11. Poisson's ratio model Cross-section, Un-interpreted and Interpreted
Figure 12. Seismic Reflection Stack using P-wave Data
Figure 13: Summary Borehole Logs, PT-1 and PT-2
Figure 14. Borehole Cross-sectoin A-A'
Figure 15. Interpreted Location of Piedmont Reverse Fault, Constrained from Geophysics and Borehole Data
Figure 16. Conceptual Model of Piedmont Reverse Fault

LIST OF APPENDICES

Appendix A. Borehole logs from Sausal Creek Restoration Project in Dimond Canyon Park Oakland, California
Appendix B. Borehole Logs for PT-1 and PT-2

1.0 INTRODUCTION

Earthquakes on the Hayward fault represent the most significant seismic hazard to the East Bay region of the greater San Francisco Bay area. The fault has been assigned a 30% probability of a ≥ M6.7 event between 2014 and 2043 (WGCEP, 2013). An earthquake of this magnitude will produce strong ground shaking throughout the Bay area, extensive liquefaction along the Bay margin, earthquake-induced slope failure throughout the East Bay Hills, and permanent ground rupture through the densely urbanized East Bay area.

Primary active strands of the Hayward fault have been mapped in detail based on prominent geomorphic features and evidence of active creep (Radbruch-Hall, 1974; Herd, 1978; Lienkaemper, 1992; Graymer et al., 1995; and others); however, secondary structures are not as well constrained. Secondary structures include multiple sub-parallel traces within the main fault zone, and relevant to this work, splays off of the main trace that appear to accommodate convergent stresses via reverse fault motion (Figure 1). The lack of attention to these structures may be partially attributed to the erasure of geomorphic evidence by active hillslope processes and urbanization. Their existence, however, is predicted by other studies. For example, recent evaluation of the Ashland fault, a thrust splay located in San Leandro (Rubin, 2011), shows evidence of Holocene activity prompting the California Geological Survey to include the fault on the Alquist-Priolo (A-P) Earthquake Fault Zone map (CGS, 2012). Inclusion of this fault into the A-P zone highlights the hazard associated with secondary (non-seismogenic[1]) thrust splays and potential risks introduced due by scientific uncertainties related to their urban location.

This collaborative pilot study investigated the Piedmont thrust, referred to herein as the Piedmont reverse fault (PRF), a potential splay of the Hayward fault in an area of anomalously high topography west of the Hayward fault in Piedmont and north Oakland, California (Figure 1). In the near surface, the PRF juxtaposes Late Cretaceous sandstone (of the Novato Quarry terrane of Blake and others, 1984) against an older Pleistocene alluvial fan unit along much of its mapped length, suggesting west-vergent thrusting as a likely mechanism (Figure 2; Graymer et al., 1995; Graymer 2000; 2005). The contact between these units has been mapped as a thrust fault by Graymer et al. (1995) and Graymer (2000) and modeled as such in Phelps et al. (2008).

Studies of recent surface ruptures and major earthquake events (1989 Loma Prieta; 2010 El Mayor-Cucapah) indicate that pre-existing fault structures can be (re)activated to accommodate oblique slip (Marshall et al., 1991; Valensise and Ward, 1991; Wei et al., 2011; Oskin et al., 2012). We hypothesize that a large earthquake on the main trace of the Hayward fault may produce co-seismic surface displacements on the PRF similar to the Holocene activity documented on the Ashland fault to the southeast.

Co-seismic (re)activation of the investigated Piedmont reverse fault during a major Hayward fault earthquake could disrupt infrastructure in the heavily urbanized area of

[1] The term non-seismogenic is used as being incapable of producing earthquakes of engineering significance, generally >M5

North Oakland as well as create significant economic damages through permanent ground deformation.

This Pilot study is designed to: (1) demonstrate the physical presence or absence of a fault that is mapped as the boundary between the Cretaceous bedrock and Pleistocene alluvial fans as shown on some published maps, and (2) constrain the location of the fault (if present) in this urbanized setting. This Pilot study integrated three lines of independent evidence via one surface and two subsurface investigative techniques: (1) geomorphic analysis of LiDAR data, (2) a focused seismic reflection and tomography survey, and (3) an exploratory borehole program coupled with existing borehole data. The Pilot study was undertaken in and near the Dimond[2] Canyon Park in Oakland, California.

[2] The correct spelling is indeed "Dimond"

2.0 TECTONIC SETTING AND PREVIOUS WORK

The Hayward fault zone is a broad zone of deformation, within which the style and location of deformation has changed through the history of the fault. Various geologists have mapped faults in the low hills between the main trace of the Hayward fault and the western margin of the East Bay Hills (e.g., Radbruch-Hall, 1969; Radbruch-Hall, 1974; Graymer et al., 1995; Graymer, 2000; Dibblee and Minch, 2005). Graymer et al. (1995) identified a zone of thrust faults west of the main Hayward fault on the basis of bedrock lithology and structure, and he shows the westernmost traces as a concealed thrust fault beneath Pleistocene alluvial fans along strike to the northwest (Figure 2). The zone consists of west-vergent imbricate thrust sheets along prominent topographic breaks-in-slope (Graymer et al., 1995). Individual faults within the zone bound Jurassic and Cretaceous rocks of the Franciscan Complex and Coast Range Ophiolite and juxtapose these terranes against and/or over Quaternary alluvium. These structures represent "accreted and deformed remnants of arc-related Jurassic oceanic crust and…turbidites" (Graymer, 2000). The bounding faults are generally sub-parallel to the strike of the Hayward fault main trace and dip toward it at an unknown angle. These faults have been mapped as such by Graymer et al. (1995), Graymer (2000), Dibblee and Minch (2005), and Phelps et al. (2008), however other maps - Graymer et al. (2006), for example - have shown some of these faults as geologic contacts, illustrating conflicting representations of the presence or absence of a tectonic fault; a critical uncertainty for seismic hazard in the East Bay.

While these thrust splays may have been first established as Mesozoic structures, there is evidence that they can re-activate and accommodate Holocene activity, as exemplified by the Ashland fault. The Ashland fault zone is located approximately 10 km (6 mi.) south of the study area (Figure 1). It bounds an area of high topography west of the main trace of the Hayward, juxtaposing Jurassic gabbro over Holocene soil and alluvium (Rubin, 2011;). The Ashland fault has been classified as active (using CGS criteria) and added to the A-P maps (CGS 2012) highlighting the potential hazard associated with subsidiary thrust splays. Little is known regarding the specific demonstration of the postulated PRF, let alone its geometry, structural kinematics, and activity; however, it superficially displays similar geomorphic and tectonic characteristics as the active Ashland fault zone; yet, it also shares similar geological characteristics as Albany Hill and Point Richmond hills.

3.0 DIMOND CANYON PARK INVESTIGATION SITE

Dimond Canyon Park is a park owned by the City of Oakland and centered on Sausal Creek. It includes the creek canyon, which is incised into the high topography west of the Hayward fault, as well as an area of more gentle topography west of the PRF (Figure 2). Sausal Creek traverses the park from northeast to southwest, decreasing in elevation from approximately 58.5 to 56.1 m amsl (192 ft. to 184 ft.). Topography surrounding the creek consists of a gently sloping, relatively planar surface that decreases in elevation from the northeast to the southwest across the park, from approximately 62.4 m to 58.5 m (205 ft. to 192 ft.). Higher topographic surfaces bound the creek to both the east and the west, with elevations ranging from approximately 73.2 to 82.2 m (240 to 270 ft.).

Mapped geologic units within the study area consist of late Cretaceous sandstones (of the Novato Quarry terrane of Blake and others, 1984), Pleistocene to Holocene alluvial fan deposits (Graymer et al., 1995, Witter et al., 2006), as well as apparent terrace deposits of Sausal Creek. Witter et al. (2006) also map artificial fill along Sausal Creek, where the watercourse is buried in a storm drain through the south end of the park.

Bedrock outcrops of the Novato Quarry terrane sandstone are mapped to the north, east, and west of Sausal Creek and coincide with higher topography adjacent to and within the park (Graymer et al., 1995; Witter et al., 2006) (Figure 3). Holocene fan complexes and alluvial deposits, mapped by both Graymer et al. (1995) and Witter et al. (2006), coincide with the gently south-southwest sloping surfaces on the northwest and southeast margins of Sausal Creek. Additionally, Witter et al. (2006) mapped early to late Pleistocene fan deposits coincident with the higher topography southwest and southeast of the park (Figure 3).

In addition to surficial geologic mapping, exploratory boreholes, collected as part of the Sausal Creek Restoration Project (Fugro, 2011), provide useful subsurface geologic information at the site. The exploratory boreholes document subsurface deposits at five locations within the park to maximum depths of 6.1 m (20 ft.) (Appendix A). Weathered bedrock was identified in borings B-3 and B-5. Observed deposits from the boreholes consist of interbedded layers of sandy lean clays, clayey sands, clayey sands with gravel, and decomposed bedrock. Sandy lean clays and clayey sands were documented from the ground surface to maximum depths of approximately 5.5 m (18 ft.). Deposits of clayey sand with gravel were intermittently documented underlying the sandy lean clay and clayey sands at depths ranging from approximately 2.1 to 4.2 m (7 to 14 ft.). The deposits of clayey sand with gravel extended to maximum depths of approximately 6.1 m (20 ft.). Two boreholes also documented decomposed sandstone and siltstone at approximate depths of 5.2 to 5.5 m (17 to 18 ft.) (Appendix A).

Cumulatively, the geomorphology and surface and subsurface geology at the site indicate a bedrock high to the north and lower topography to the south, underlain by Pleistocene to Holocene alluvial fan deposits.

4.0 APPROACH AND METHODOLOGY

To provide preliminary constraints on the PRF, we performed three primary tasks. Task 1 focused on desktop efforts to compile and review existing data regarding the fault; Task 2 consisted of collecting and analyzing high-resolution seismic reflection and tomography data across the fault in Dimond Canyon Park; and Task 3 involved the collection and documentation of subsurface sediments from exploratory boreholes in the hanging-wall and footwall of the fault in Dimond Canyon Park.

4.1 Compilation and Review of existing data

Prior to field activities, we compiled published peer-reviewed literature, geotechnical reports, aerial photography, historical topographic maps, and LiDAR data. Existing geotechnical borehole data for Dimond Canyon Park were obtained and reviewed to provide preliminary stratigraphic control and constrain geologic relationships in the site vicinity.

Alameda County LiDAR data were input into GIS to construct a high-resolution digital elevation model (DEM), as well as derivative GIS maps (i.e. hillshade and slope maps) of the study area. The digital elevation model and LiDAR hillshade and slope maps were used to construct fault perpendicular profiles to examine and document the geomorphic expression of the fault. Profiles were evaluated for evidence of gradient changes or disruptions to help assess possible prehistoric activity on the PRF, as well as assess the geometry and magnitude of deformation across the fault. We used the initial results from this analysis to guide the location of the seismic survey line in Dimond Canyon Park.

4.2 Seismic Data Collection

To better determine the location and shallow-depth geometry of the PRF, we used high-resolution seismic imaging methods described by Catchings et al. (2014) to develop tomographic models of P- and S-wave velocity and P-wave reflection images.

In February 2015, we acquired high-resolution P- and S-wave seismic data along a 2-D profile across the mapped trace of the PRF at Dimond Canyon Park in Oakland (Figure 3). The final location of the seismic line was revised from the proposal due to potential interference from subsurface structures such as culverts, water pipes, and building foundations. Our seismic profile was 315 m (1,030 ft.) long, trending southwest to northeast (Figure 3). P and S-wave data were acquired separately using hammer sources (shots) consisting of vertical (for P-wave) and horizontal (for S-waves) hammer blows, respectively, on steel plates. Each shot was co-located with a geophone, and all P- and S-wave shots were recorded by 106 P-wave (40-Hz) and S-wave (4.5-Hz) geophones, respectively. The spacing between geophones was 3 m (10 ft.). All data were recorded using two Geometics RX-60 multi-channel seismograph systems (each with 60 channels) that were connected to refraction cables. We recorded the data in two phases. First, we deployed vertical-component sensors along the seismic profile, and we used vertical hammer blows (P-wave shots) at each sensor to record P-wave data along the entire array, thereby using a total of 106 shot points, each recorded by 106 sensors for the P-wave data set. We then substituted the horizontal-component sensors for the vertical-component sensors, and we

used horizontal hammer blows (S-wave shots) at the same shot points, thereby using a total of 106 shot points, each recorded by 106 sensors for the S-wave data set.

By using 106 shots that were each recorded by 106 sensors, the P- and S-wave data sets each consisted of approximately 11,236 traces along the 315-m-long seismic profile. The density of the data allows for the high redundancy needed for both tomographic modeling and reflection stacking. The P-wave data were recorded with vertical-component geophones, as such the data consist dominantly of compressional (P) body waves and its associated surface (Raleigh) waves (Figure 4). Similarly, the S-wave data were recorded with horizontal-component geophones, which yield data that dominantly consist of Love waves (Figure 5).

The acquisition geometry allowed us to develop multiple types of seismic models and images, including (a) P-wave refraction tomography, (b) P-wave reflection images, (c) S-wave refraction tomography, (d) S-wave reflection images (optional), (e) Vp/Vs ratio models, and (f) Poisson's ratio models. The refraction tomography models were developed using the code of Hole (1992), and the reflection data were processed using an interactive data processing package known as ProMax.

4.3 Borehole Data Collection

Preliminary results from the geophysical data collection were used to provide location constraints for the borehole program. The borehole program provided geologic constraints on the seismic survey profiles and stratigraphic control for the study area in Dimond Canyon Park. Additionally, the boring data collected for this study were integrated with data obtained from previous work to construct an integrated stratigraphic framework for the study area and constrain the geologic relationships for the PRF.

The subsurface exploration program completed by Fugro, Inc. in August of 2015 consisted of two boreholes; one in the presumed hanging-wall and the second in the presumed footwall of the fault. A total of 32 m (103 ft.) were drilled for this study. Boreholes were completed with a CME D72 track mounted rig and continuously sampled predominantly utilizing a 101 mm inner diameter (4-inch) Geobore sampler, but also a 152 mm (6-inch) bucket auger, and a 51 mm (2-inch) outer diameter split spoon sampler as Standard Penetration Tests (SPTs) in accordance with ASTM 1586. In addition to being cleared by Underground Service Alert, borehole locations were hand cleared in the field to 1.8 m by using a T-probe and advanced to that depth with the bucket auger. Boreholes were completed in accordance with local and federal laws, codes, and standards of practice. Michael Buga of Fugro, Inc. logged both borings collected for the pilot study. All recovered samples were classified in accordance with ASTM D2487 and D2488. Samples were photographed, bagged, labeled, and boxed. Borehole logs are presented in Appendix B.

5.0 ANALYSIS AND RESULTS

The results from each task - LiDAR analysis, seismic survey, and borehole program - were used to constrain and refine the potential location and character of the PRF. The individual results from these tasks are presented and discussed below. A summary of the results is presented in subsection 4.4.

5.1 Fault Perpendicular LiDAR Profiles

Four fault perpendicular profiles were derived from Alameda County LiDAR data across the mapped trace of the fault (Grayer, 2000) to document any gradient changes and disruptions across the structure (Figure 6). The fault trace of Graymer et al. (1995) is located on each profile. This fault trace should be considered approximate, based on the small scale at which it was mapped versus the scale of the image. Uncertainties in location because of scale differences may be as much as 300 m (1,000 ft.).

Profile 1 crosses the southern end of the mapped fault in Dimond Canyon Park. Profile 1 (Figure 7) documents a prominent 21 m (70 ft.) down-to-the-southwest slope break in Dimond Canyon Park. The fault is mapped approximately 32 m (105 ft.) to the northeast of the base of the slope break, part way up the slope.

Profile 2 is located at the eastern margin of the Pleistocene alluvial fan immediately west of the park and extends along a north-northeast-south-southwest trend. Profile 2 shows a subtle 7 m (20 ft.) down-to-the-southwest slope break at approximately 360 m (1,200 ft.) along the profile. The fault trace is mapped approximately 33 m (110 ft.) to the northeast and does not correlate well with the apparent slope break. However, the difference between the location of the slope break and the mapped fault may reflect the small scale at which the structure was originally mapped, and the lack of available high-resolution elevation data.

Profiles 3 and 4 follow the high topography associated with the Pleistocene alluvial fan deposit to the northwest of Trestle Glen Creek, approximately 600 m (1 mi.) northwest of the park. Profile 3 documents subtle slope breaks at approximately 330 m (1,100 ft.), 360 m (1,200 ft.), and 430 m (1,400 ft.) respectively along the profile. The western most slope break represents an approximately 7 m (20 ft.) down-to-the-west slope break that generally coincides with the fault, with the mapped trace approximately 30 m (100 ft.) to the west. Similar to Profile 2, the scale at which the structure was originally mapped and the resolution of the available data may account for the slight difference between the location of the slope break and the fault.

Profile 4 documents a subtle 10 m (40 ft.) down-to-the-west slope break at approximately 310 m (1,020 ft.) along the profile, about 40 m (130 ft.) to the east of the mapped fault. The subtlety of the slope break, and the lack of available high-resolution elevation data when the fault was originally mapped may account for the slight difference between the two features.

Cumulatively the fault perpendicular profiles document a slope break that generally coincides with the mapped trace of the fault by Graymer et al. (1995), with the difference between the mapped trace and the slope break ranging from 7 to 21 m (20 ft. to 70 ft.). The scale at which the original fault was mapped, and the lack of available high-resolution elevation data may account for the minor discrepancies between the mapped trace of the fault and the observed slope break.

5.2 High resolution P- and S-wave seismic data

High-resolution seismic imaging methods described by Catchings et al. (2014) were used to develop tomographic models of P- and S-wave velocity and P-wave reflection images. These coincident P- and S-wave velocity models were further used to develop tomographic models of Vp/Vs and Poisson's ratio, which are sensitive to shallow-depth faulting. We also compare 2-D surface-wave measurements of S-wave velocity structure with those measurements determined from refraction tomography to assess the presence or absence of a PRF in the vicinity of Dimond Park.

5.2.1 P-Wave Refraction Tomography Velocity Model

We developed a P-wave refraction tomography velocity model from first-arrivals measured on P-wave shot gathers using the algorithm of Hole (1992). We inverted the velocity model using a 3-m by 3-m grid and up to 11,236 first-arrivals, which allowed for a high degree of redundancy and resolution within the model. Our starting models were developed from 1-D analysis of shot gathers along the profile. We used multiple starting models, but all final models were similar, with less than about 2% variation among the models where best resolved. Our preferred final model is shown in Figure 8. The P-wave velocities range from about 600 -2100 m/s on the southwestern side of the profile, but P-wave velocities are considerably higher on the northeast side, ranging from about 800 -3200 m/s. There is a clear near-vertical discontinuity in velocities from the northeast to the southwest side of the profile, with the discontinuity occurring between meters 150 and 160 of the seismic profile, where there is also a prominent topographic peak at the surface. In this report, we interpret this prominent near-vertical velocity discontinuity, which coincides with other seismic anomalies discussed below, to be the a major trace of PRF in the upper 50 m. At depths below about 50 m, higher P-wave velocities extend southwest of the 150- to 160-m range. However, we suggest that the higher P-wave velocities at that depth likely represent the top of the vertically offset rocks seen on the northwestern side of the fault (Figure 8). There is also an offset in the 1500 m/s velocity contour, which has been shown to coincide with the top of static ground water in numerous studies (see Catchings et al., 2014 for a summary), across our interpreted fault. The offset in the inferred depth to the top of ground water suggests that this trace of the PRF is a ground-water barrier.

5.2.2 S-Wave Refraction Tomography Velocity Model

We developed an S-wave refraction tomography velocity model from first-arrivals measured on the S-wave shot gathers (Figure 9), also using the algorithm of Hole (1992). As with the P-wave model, we used a 3-m by 3-m grid and a large number of the 11,236 S-wave first-arrivals that were available, which similarly allows for a high degree of redundancy and resolution for the S-wave model. Because first-arrivals for the longer offset traces were contaminated with cultural (dominantly traffic) noises, we opted not to use a

number of the longer offset arrivals. This resulted in a shallower depth of S-wave imaging than with the P-wave arrivals.

For S-wave modeling, we also used multiple 1-D starting velocity models as input to the tomographic inversion. However, each starting model yielded a similar final model, suggesting that the model is well resolved. Our preferred 2-D S-wave model is shown in Figure 9. S-wave velocities range from about 260-520 m/s on the southwest side of the profile to about 500-800 m/s on the northeast side. As with the P-wave velocity model, there is a sharp transition from the higher S-wave velocities on the northeast to the lower S-wave velocities on the southwest, which occurs along a near-vertical discontinuity centered near meter 160, beneath a prominent topographic peak. Because of the sensitivity of S-waves to the rigidity of lithologic units, we suggest that the tomographic S-wave velocity model best illustrates the faulted discontinuity between the sandstone (of the Novato Quarry terrane of Blake and others, 1984) and the older Pleistocene alluvial unit. This suggests that this trace of the PRF is dominantly near vertical (~80 to 85 degrees) in the upper few tens of meters at Dimond Park, and it is centered between meters 150 and 160 near the surface along our seismic profile.

5.2.3 Vp/Vs Model

Using the method described by Catchings et al. (2014), we developed models of Vp/Vs ratios along the seismic profile (Figure 10). Because we used the same model parameters and profile geometry for the P- and S-wave velocity models, Vp/Vs models along the profile could be developed by dividing the P-wave velocity by the S-wave velocity at each node of the velocity models. However, because the maximum depth of tomography imaging was shallower for the S-wave model than the P-wave model, we could develop the Vp/Vs ratio model only to the maximum depth of the S-wave model.

Vp/Vs ratios range from about 1.6 to about 4.2, with the lowest ratios in the near-surface at the topographic high near the center of the seismic profile and the highest values to the southwest and northeast ends of the profile. A prominent area of low Vp/Vs ratios near meter 150 (beneath the topographic high) is observed at 10 to 15 m below the surface. This low value is oriented near vertically, with a slight northeasterly dip (~79°). We suggest that the Vp/Vs model is more sensitive to the fault structure at depths greater than about 20 m than either the Vp or Vs model. Thus, the dip of the fault, as inferred from the Vp/Vs model, is likely about 80 degrees at about 20 m depth.

5.2.4 Poisson's Ratio Model

In a manner similar to that for Vp/Vs ratios, we used the P- and S-wave velocity models to develop a model Poisson's ratio ($= V_P^2 - 2V_S^2 / 2(V_P^2 - V_S^2)$) along the seismic profile (Figure 11). Poisson's ratio varies from about 0.2 near the surface beneath the central topographic high to about 0.47 near the southwest and northeast ends of the profile at about 20 to 40 m below the surface. Poisson's ratio for materials can vary widely, but the maximum value of 0.5 typically correlates with a fluid. There is a region of relatively low Poisson's ratios directly beneath the topographic high, near the center of the seismic profile. Because shallow-depth Poisson's ratios of about 0.43 have been shown to correlate with highly water-saturated materials (Catchings et al., 2014), our model suggests the fault along the central part of our seismic profile (fault zone) is water saturated only at depths greater than about 40 m, but areas to the southwest and northeast are water saturated at relatively

shallow depths (as low as 3 m on the SW and 8 m on the NE). The shallow-depth highly saturated zones inferred from Poisson's ratio differs from the top of groundwater inferred above from the V_p = 1500 m/s contour (which does not show the prominent low at the fault zone) because the lower resolution of the P-waves may not image a relatively narrow zone of low velocities (fault) at depths of several tens of meters. The relatively shallow zones of high saturation (high Poisson's ratio) likely arise from watering of the grass in Dimond Park, particularly to the southwest, but those shallow zones probably do not reflect the depth to the static ground water level. The relatively low Poisson's ratio values at the fault further suggest that the fault acts as a barrier to groundwater flow.

5.2.5 Seismic Reflection Images

We developed a seismic reflection stack of the data using the P-wave data from our seismic survey (Figure 12). Semi-continuous reflections are observed along the southwestern part of our seismic profile (between distance meters 0 and 75, within upper 50 m depth), which consists of older Pleistocene alluvium, but continuous reflections are largely absent along the northeastern part of our seismic profile (meters 140 to ~300), which consists of the dominantly disrupted and variably dipping sandstone. This variation in reflectivity suggests that the rocks beneath the northeastern part of the seismic profile are not well layered or are not continuously sub-horizontally layered, which is consistent with geologic mapping in the area. According to Graymer et al. (1995), the dip of the sandstone unit in our immediate study area varies from about 57 degrees southwest to about 50 degrees northeast, and within hundreds of meters of our seismic line, dips vary even more widely from about 80 degrees southwest to 65 degrees northeast. In addition, northwest and easterly dips are also observed and range up to 85 degrees. Thus, we would not expect highly resolved reflection images along our seismic profile.

We do, however, observe reflection evidence for structures that are consistent with the mapped geology in the area. Near the southwestern end of the profile, the surface geology consists of Holocene fan and fluvial deposits, which are presumably overlie Pleistocene alluvial fan and fluvial deposits. There is little topography associated with these deposits along the southwestern end of the seismic profile, suggesting that they should be dominantly sub-horizontally layered deposits. On the southwestern end of the seismic reflection image, we observe sub-horizontal reflectors in about the upper 40 to 50 m, underlain by northeasterly to sub-horizontally dipping reflectors.

Near the center of the seismic profile (~ meter 158), geologic mapping (Figure 2) suggests northeastward dipping (~ 50 degrees) strata, and we similarly observe northeastward dipping reflections on our seismic image. North of the northern end of our seismic profile, geologic mapping (Figure 2) suggests southwest-dipping (~57 degrees) strata, and we similarly observe southwestward dipping strata on the seismic reflection image. The large variations in strike, dip, and lithology, however, suggest that laterally continuous reflections are unlikely to be observed along the length of our seismic profile. In addition, there are prominent diffractions in places along the seismic profile, particularly near the central part of the seismic profile (meters 150 to 160) and several locations (meters 200-250 and near meter 300) to the northwest. These diffractions further distort the reflection image. Such diffractions, which can be seen to at least 300 m depth, typically coincide with disruptions in rock strata, such as offsets caused by faulting or intrusions. To better understand the

cause of the diffractions observed along our seismic profile, we superimposed our S-wave tomography image on our reflection image to better interpret the reflection image (Figure 12).

We compare the S-wave tomography image because S-wave velocities a more sensitive to the rock type (rigidity), but P-wave velocities are more sensitive to groundwater (Figure 12). The combined S-wave velocity/ reflection image shows that diffractions correlate with the major lateral change in velocity between meters 150 and 160 of the seismic profile, further suggesting that the trace of the PRF is located in the 150 to 160 m distance range of our seismic profile.

5.3 Footwall and Hanging-wall Exploratory Borings

Two exploratory boreholes were drilled within the park to provide stratigraphic constraints on the seismic data, provide direct geologic samples, potentially provide dateable material (detrital charcoal), and assess the presence of Holocene deposits as well as potential stratigraphic offset.

Borehole PT-1 was located on the hanging-wall of the fault in the vicinity of Sausal Creek to further constrain the location of the fault zone, examine the subsurface stratigraphy, and assess the potential for trenching in Holocene deposits. Its location was chosen between the previously drilled Fugro boreholes and the projected location of the fault from the seismic survey to further constrain the location of the PRF in the stream valley. The second borehole, PT-2, was located on the footwall of the fault along the western end of the seismic line to provide constraints on stratigraphy imaged by the seismic survey and provide additional constraints on the location of the fault zone.

5.3.1 Hanging-wall Boring (PT-1)

Borehole PT-1 was drilled to 6.4 m (21 ft.) and terminated in weathered siltstone (Figure 13). Fill material was documented to a depth of 1.9 m (6.2 ft.), and consisted of dry, dark yellowish silty clay with gravel. The gravel consisted of sub-angular sandstone clasts up to 25.4 to 50.8 mm (1- to 2-in.) in diameter. Underlying the fill material was a dark gray to black clay with sand and gravel to a depth of 2.7 m (9.0 ft.), which was subsequently underlain by clayey sand to a depth of 4.7 m (15.5 ft.). A lens of gravelly sand within the clay was documented from 4.66 to 4.72 m (15.3 to 15.5 ft.) at the base of the clayey sand package. Beneath the clayey sand layer from 4.7 to 5.5 m (15.5 to 18.0 ft.) a yellowish brown fine to medium gravel with clay and sand was documented. Underlying the gravel with clay and sand was dark gray siltstone gravel with clay, interpreted as weathered siltstone bedrock with clay seams. The materials beneath the fill layer are stiff and contain a significant amount of clay. Their appearance suggests that they are at least early Holocene, but more likely Pleistocene in age.

Historical photos of the park indicate that the fill material documented from the ground surface to 1.9 m (6.2 ft.) is likely associated with the original grading of the park and installation of the culvert. The clay with sand and gravel and the clayey sand documented between 1.9 to 4.7 m (6.2 and 15.5 ft.) indicate a depositional environment with moderate

to low energy based on the presence of intermittent gravels, and likely represent deposits from the creek and/or colluvium from the slope. The gravel documented between 4.7 to 5.5 m (15.5 and 18.0 ft.) indicate a depositional environment with higher energy likely reflecting channel deposits associated with the creek. Additionally, the depth to the interpreted channel gravels documented in PT-1 coincide with depths to similar gravel deposits documented in boreholes for the Sausal Creek Restoration Project (Figure 14). The interpreted channel deposits overlie and are incised into the weathered siltstone with clay seams. The bedrock documented in PT-1 coincides with bedrock depths documented in boreholes for the Sausal Creek Restoration project.

5.3.2 Footwall Boring (PT-2)

Borehole PT-2 was drilled to a total depth of 25 m (82 ft.), where borings were collected at approximately meter 62 along the seismic line (Figure 13). Fill material was documented to a depth of 2.6 m (8.4 ft.), and primarily consisted of dark yellowish brown sandy silt with gravel. Beneath the artificial fill at 2.6 m (8.4 ft.) samples consisted of yellowish brown clay and sandy clay with varying amounts of gravel, to a depth of 6 m (19.7 ft.) From 6 m (19.7 ft.) to a depth of 9.9 m (32.4 ft.), collected samples consisted of reddish, yellowish brown sandy clay with trace gravel. Additionally, a root was noted at a depth of 6.2 m (20.3 ft.). At 9.9 m (32.4 ft.) a gradational color change from reddish, yellowish, brown to a bluish gray was observed; the bluish gray clay continued to a depth of 11.7 m (37.3 ft.) (Appendix B). Underlying the bluish gray clay, a greenish gray, clayey, angular to sub-angular gravel was documented between 11.4 and 11.7 m (Figure 13; 37.3 and 38.5 ft.). Beneath the clayey gravel to a depth of 19.9 m (65.4 ft.), the observed samples consisted of sandy clay with interbedded sand and gravel, ranging in thickness from approximately 5 to 15 cm (2 to 6 in.)(Appendix B). Samples collected from 19.9 m (65.4 ft.) to the bottom of the hole consisted of clay with occasional sandy interbeds. The gravel and sand content of the clay increased with depth from 24.2 m (79.4 ft.) to the bottom of the hole at 25 m (82 ft.).

Similar to PT-1, the fill material documented between the ground surface and 2.6 m (8.4 ft.) likely relates to the original grading of the park, and in this particular case, a buried storm water drain. We interpret the deposits of clay and sandy clay that underlie the fill between 2.6 m to 11.4 m (8.4 and 37.3 ft) likely represent a low energy depositional environment, and may reflect overbank deposits from the Sausal Creek (Figure 14). Occasional gravel deposits documented within the clays could represent storm event deposits from Sausal Creek or slope derived colluvium. The root observed at a depth of 6 m (19.7 ft.) within the sandy clay suggests the presence of a buried soil horizon.

Underlying the clay and sandy clay is a deposit of 30 cm (11 in.) thick greenish gray angular to sub-angular clayey gravel between 11.4 and 11.7 m (37.3 to 38.5 ft.). We interpret the clayey gravel to represent a colluvial deposit based on the angularity of the clasts. The thickness of the gravel deposit is anomalous relative to the overlying material, suggesting it is not related to Sausal Creek. Although speculative, we suggest the observed gravel deposit could represent colluvium deposited as a result of strong ground shaking (Figure 14).

There is also a color change at approximately 10 m in the sandy clay from a reddish, yellowish, brown to a bluish gray indicating a reducing environment, which could represent a zone of relatively high groundwater flow (Figure 14). The color change is unique to the borehole at this depth and is of a significant thickness, extending from a depth of approximately 10 to 11.8 m (32 to 39 ft). Typically, ground water flows along the top of an aquitard, which suggests the presence of more consolidated material below approximately 11.8 m (39 ft.).

Additionally, the deposits between about 2.6 and 11.7 m (8.4 and 38.5 ft) correlate with a zone of relatively low S-wave velocities between distance meter 40 and 100, as shown by the relative low in the 350 m/s contour (Figure 9). The zone of low S-wave velocities suggests the clay and sandy clay, as well as clayey gravel observed between 2.6 and 11.7 m (8.4 and 38.5 ft.) are less rigid relative to the nearby materials, and thus may represent relatively younger, less consolidated deposits (i.e. overbank and colluvial material).

Underlying the angular to sub-angular clayey gravel is a light brown clayey sand from 11.7 m (38.5 ft.) to 19.9 m (65.4 ft.) with interbedded sandy gravel, clayey gravel and sandy clay. Additionally, sandstone and chert lithics, as well as abundant chert gravels, were documented at depths of 13.7 m (44.9 ft.), 16.3 m (53.4 ft.), and 16.8 m (55 ft.)(Appendix B). The presence of sandstone and chert lithics, as well as abundant chert gravels at and below 13.7 m (44.9 ft.) may represent in-situ weathered bedrock. However, based on the relatively low seismic velocities in both the P- and S-wave models at these depths, we interpret that the gravels and lithics represent colluvial material derived from the adjacent slope and coarser Pleistocene alluvial deposits.

Underlying the clayey sand at a depth of 19.9 m (65.4 ft.) is a massive brown to olive gray clay to a depth of 24.2 m (79.4 ft.). At 19.9 m (65.4 ft.) the clay is highly weathered to residual soil and may represent a buried soil horizon. Interbeds of clayey sand and sandy clay were observed at depths of 20.9 m (68.8 ft.), 21.3 m (70 ft.), 21.9 m (72 ft.), 22.6 m (74.2 ft.), and 23 m (75.4 ft.)(Appendix B). The generally massive nature of the clay observed between 19.9 m (65.4 ft.) and 24.2 m (79.2 ft.) suggests it may represent weathered Franciscan mélange, possibly a highly weathered shale. This interpretation would suggest a vertical separation in bedrock of approximate 15 m (49 ft.) across the PRF between PT-1 and PT-2. However, because the interpreted bedrock in PT-2 (weathered shale) was not observed in PT-1 (siltstone with clay seams), or the boreholes collected from previous studies, the vertical separation measurement represents a minimum, or it suggests that bedrock is deeper than ~20 m on the southwest side of the fault. Alternatively, the interbeds of clayey sand and sandy clay suggest the deposit could have an alluvial origin.

A gravelly lean clay underlies the massive brown to olive gray clay from 24.2 m (79.4 ft.) to the bottom of the hole at a depth of 25 m (82 ft.). The gravel and sand content increase with depth to 24.7 m (81 ft.), where it is a gravelly sand with clay. The gravel documented from 24.2 m (79.4 ft.) to the bottom of the hole may represent clasts of in-situ weathered bedrock, or alternatively higher energy deposits associated with an alluvial fan.

Interpretations of the P-wave velocity model and the seismic reflection image by Catchings et al. (2016) suggest the Novato Quarry sandstone could be as deep as 40 to 50 m (130 to 160 ft.) in the vicinity of PT-2, beyond the depth of the borehole. This interpretation would suggest a vertical separation in the bedrock of 35 to 45 m (135 to 150 ft.) across the PRF. Although differing in magnitudes, both data sets suggest a vertical separation in bedrock across the fault.

6.0 SUMMARY OF FINDINGS

Results from this Pilot study are summarized as follows:

- The fault perpendicular LiDAR profiles document slope breaks clearly expressed across Pleistocene and Holocene fan deposits and ranging in magnitude from 7 to 21 m (20 to 70 ft.).
- The slope breaks generally coincide with mapped trace of the fault by Graymer et al., (1995), although the scale at which the original fault was mapped and the lack of available high-resolution elevation data at that time likely account for the minor discrepancies between Graymer's mapped trace of the fault and our observed slope break.
- The tomographic S-wave velocity model appears to image a faulted discontinuity between deposits of contrasting rigidity. This suggests that the main trace of the PRF is dominantly near vertical (~80 to 85 degrees) in the upper few tens of meters at Dimond Canyon Park, and it is centered between meters 150 and 160 near the surface along the S-wave seismic profile (Figure 9).
- The Vp/Vs model (Figure 10) is slightly more sensitive to the fault structure at depths greater than about 20 m than either the individual Vp or Vs model, and based on a prominent area of low Vp/Vs ratios near meter 150 (beneath the topographic high), it further suggests the dip of the PRF at 10 to 15 m below the surface (about 80 degrees at 20 m depth);
- The relatively low Poisson's ratio values (Figure 11) further suggest the presence of a fault that also appears to act as a barrier to deep groundwater flow.
- Prominent diffractions are imaged in places along the seismic profile (Figure 12), particularly near the central part of the seismic profile (meter 150 to 160) and several locations to the northwest. Typically, such diffractions coincide with disruptions in rock layering caused by faulting or intrusions.
- The combined image of S-wave tomography, overlain on our seismic reflection image (Figure 12), shows that the diffractions correlate with the major lateral change in velocity between meters 150 and 160 of the seismic profile. This further supports the presence of PRF in the subsurface and suggests that the main trace of the PRF is located in the 150 to 160 m distance range of our seismic profile.
- Borehole data suggest a minimum vertical separation in the bedrock of approximately 15 m (49 ft.) over a distance of about 91 m (300 ft.) across the fault;
- Interpretations of the P- and S-wave model (Figure 8) and the seismic reflection image (Figure 12) suggest a vertical separation in the Novato Quarry sandstone of approximately 35 to 45 m (135 to 150 ft.);
- Both boreholes contain Pleistocene alluvium, whereas PT-1 may also include early Holocene channel deposits; and
- PT-2 may contain a colluvial deposit associated with strong ground shaking at approximately 48.5 m (159 ft.) elevation.

7.0 SIGNIFICANCE OF RESULTS

This pilot study used a desktop analysis of Alameda County LiDAR data, a focused seismic reflection and tomography survey, and an exploratory borehole program to provide initial constraints on the presence and location of the PRF. That is, targeted geologic analyses (beyond surface geologic mapping) was used to support or refute the presence of a tectonic fault west of the Hayward fault in the Piedmont area, similar to the Ashland fault to the southeast – a critical question in light of the recently documented activity of the Ashland fault. Specifically, this study focused on collecting three independent lines of evidence to further characterize the geomorphic expression and location of the PRF at the site specific scale.

All seismic velocity models (both P- and S-wave) show a near-vertical prominent change in velocity between meters 150 and 160 of the Diamond Canyon Park seismic profile. We interpret our seismic data as representing a steeply east-dipping fault, with a slight reverse component (northeast side up), that is located in the shallow subsurface between meters 150 and 160 of our seismic profile. This geometry is consistent with a conceptual model wherein the upper extents the fault imaged in this study are correlative with a positive flower structure of a splay fault that roots into the Hayward fault at some depth. This model, a left-step fault splay from a dextral system, would result in a compression, uplift, and positive topography (Figure 16). Additionally, interpretations of the geophysical data by Catchings et al. (2016) suggest the possibility of a vertical separation in the Novato Quarry sandstone of 35 to 45 m (120 to 150 ft.) across the fault.

Fault perpendicular topographic profiles, constructed from LiDAR data, show a slope break across Pleistocene and Holocene fan deposits that is proximal to the mapped trace of the fault by Graymer et al. (1995). On the higher Pleistocene alluvial surfaces between the drainages (i.e., interfluves), the slope break is subtle but still apparent as an approximately 7 to 10 m (20 to 30 ft.) down-to-the-west step in the topography. The presence of the slope break across both Pleistocene and Holocene surfaces suggests it may represent a geomorphic expression of the fault.

The borehole cross-section (Figure 14) indicates a minimum vertical separation in bedrock between PT-1 and PT-2 of approximately 15 m (49 ft.), northeast to southwest across the mapped trace of the fault over a distance of about 91 m (300 ft). The apparent elevation variation in bedrock also generally coincides with the slope break apparent in the fault perpendicular profiles (Figure 15). Collectively, we interpret that the borehole and that the topographic data suggest the possibility of a fault coincident with the slope break that extends through the park.

The unconsolidated deposits encountered in the boreholes have not been dated as part of this study. Based on geologic mapping by previous workers, the deposits are Holocene to Pleistocene in age. Their appearance and character in the recovered borehole samples suggests a similar age. This means that if there has been Holocene movement on the PRF, evidence in the form of displaced Pleistocene strata should be preserved within these deposits. Additionally, the gravels encountered in PT-1 represent channel fill and are inset to, and therefore younger than, the surrounding units, which could also potentially record

Holocene offsets from tectonic activity on the PRF. Borehole data collected for this study, as well as available data from previous studies, did not provide adequate resolution to assess the presence or lack of Holocene stratigraphic offset.

Data from both the seismic survey, as well as the borehole program, support the contention of a PRF that generally coincides with the previously mapped trace by Graymer et al. (1995). However, the steeply-dipping fault, interpreted in the seismic models, does not coincide exactly with the vertical separation in the bedrock observed in the borehole cross-section, which suggests the possibility of more than one fault strand present in the subsurface within our pilot study area.

The results of this Pilot Study also demonstrate that the seismic imaging, in this instance, is a more powerful tool to assess the presence or absence and location of a PRF fault compared to the LiDAR analyses, although those analyses have a degree of value from which to characterize (although perhaps somewhat questionably) the geomorphic evidence for the presence of a fault. The limited depth of the borehole data are permissive, but are neither conclusive nor equivocal, data from which to assess the presence of a fault.

8.0 ACKNOWLEDGEMENTS

This study was funded in part by USGS Earthquake Hazard Program Award G15AP00025. We would like to thank the City of Oakland for providing access to Dimond Canyon Park for this pilot study, as well as all Jermile Erdem, Ryan Fay, Gini Gandhok, Adrian McEvilly, and Seth Shuler for assistance in the field. Additionally, we would like to thank Janet Sowers of Fugro for providing a technical guidance during the planning stages of the project, as well as a technical review of the study results.

9.0 REFERENCES

Abrahmson, N. A., and Somerville, P. G., 1996, Effects of the hanging wall and footwall on ground motions recorded during the Northridge earthquake: Bulletin of the Seismological Society of America, v. 86, no. 1B p. 6.

Bourbie, T., Coussy, O., and Zinszer, B., 1987, Acoustics of porous media, Houston, TX, Gulf Publishing.

California Geological Survey (CGS), 2012, Earthquake zones of required investigation, Hayward quadrangle.

Catchings, R., Rymer, M., Goldman, M., Sickler, R., and Criley, C., 2014, A Method and Example of Seismically Imaging Near-Surface Fault Zones in Geologically Complex Areas Using VP, VS, and their Ratios: Bulletin of the Seismological Society of America.

Crane, R., 1988, Geologic map of the Hayward quadrangle.

Diblee, T. W., and Minch, J. A., 2005, Geologic map of the Oakland East quadrangle, Contra Costa and Alameda Counties, California: Dibblee Geological Foundation, scale 1: 24,000.

Field, E. H., Arrowsmith, R. J., Biasi, G. P., Bird, P., Dawson, T. E., Felzer, K. R., Jackson, D. D., Johnson, K. M., Jordan, T. H., and Madden, C., 2014, Uniform California Earthquake Rupture Forecast, version 3 (UCERF3)—The time-independent model: Bulletin of the Seismological Society of America, v. 104, no. 3, p. 1122-1180.

Fugro Consultants Inc., 2011, Geotechnical study, Sausal Creek Restoration Project in Dimond Park, Oakland, California.

Graymer, R., Ponce, D., Jachens, R., Simpson, R., Phelps, G., and Wentworth, C., 2005, Three-dimensional geologic map of the Hayward fault, northern California: Correlation of rock units with variations in seismicity, creep rate, and fault dip: Geology, v. 33, no. 6, p. 521-524.

Graymer, R., Sarna-Wojcicki, A., Walker, J., McLaughlin, R., and Fleck, R., 2002, Controls on timing and amount of right-lateral offset on the East Bay fault system, San Francisco Bay region, California: Geological Society of America Bulletin, v. 114, no. 12, p. 1471-1479.

Graymer, R. W., 2000, Geologic map and map database of the Oakland metropolitan area, Alameda, Contra Costa, and San Francisco Counties, California.

Graymer, R. W., Jones, D. L., and Brabb, E. E., 1995, Geologic map of the Hayward fault zone, Contra Costa, Alameda, and Santa Clara counties, California: a digital database: US Geological Survey, 2331-1258.

Graymer, R. W., Moring, B. C., Saucedo, G. J., Wentworth, C. M., Brabb, E. E., and Knudsen, K. L., 2006, Geologic Map of the San Francisco Bay Region.

Hauksson, E., Stock, J., Hutton, K., Yang, W., Vidal-Villegas, J. A., and Kanamori, H., 2011, The 2010 M w 7.2 El Mayor-Cucapah Earthquake Sequence, Baja California, Mexico and Southernmost California, USA: Active Seismotectonics along the Mexican Pacific Margin: Pure and Applied Geophysics, v. 168, no. 8-9, p. 1255-1277.

Hayashi, K., 2008, Development of surface-wave methods and its application to site investigations.

Hayashi, K., and Suzuki, H., 2004, CMP cross-correlation analysis of multi-channel surface-wave data: Exploration Geophysics, v. 35, no. 1, p. 7-13.

Herd, D. G., 1978, Map of Quaternary faulting along the northern Hayward fault zone; Mare Island, Richmond, Briones Valley, Oakland West, Oakland East, San Leandro, Hayward, and Newark 7.5-minute quadrangles, California, 2331-1258.

Hole, J., 1992, Nonlinear high-resolution three-dimensional seismic travel time tomography: Journal of Geophysical Research: Solid Earth, v. 97, no. B5, p. 6553-6562.

Li, Y.-G., and Leary, P., 1990, Fault zone trapped seismic waves: Bulletin of the Seismological Society of America, v. 80, no. 5, p. 1245-1271.

Li, Y.-G., and Vidale, J. E., 1996, Low-velocity fault-zone guided waves: numerical investigations of trapping efficiency: Bulletin of the Seismological Society of America, v. 86, no. 2, p. 371-378.

Lienkaemper, J., Borchardt, G., and Lisowski, M., 1991, Historic creep rate and potential for seismic slip along the Hayward fault, California: J. geophys. Res, v. 96, no. 18, p. 261-218.

Lienkaemper, J. J., 1992, Map of recently active traces of the Hayward fault, Alameda and Contra Costa counties, California.

Lienkaemper, J. J., McFarland, F. S., Simpson, R. W., Bilham, R. G., Ponce, D. A., Boatwright, J. J., and Caskey, S. J., 2012, Long-term creep rates on the Hayward fault: Evidence for controls on the size and frequency of large earthquakes: Bulletin of the Seismological Society of America, v. 102, no. 1, p. 31-41.

Marshall, G. A., Stein, R. S., and Thatcher, W., 1991, Faulting geometry and slip from co-seismic elevation changes: The 18 October 1989, Loma Prieta, California, earthquake: Bulletin of the Seismological Society of America, v. 81, no. 5, p. 1660-1693.

Oskin, M. E., Arrowsmith, J. R., Corona, A. H., Elliott, A. J., Fletcher, J. M., Fielding, E. J., Gold, P. O., Garcia, J. J. G., Hudnut, K. W., and Liu-Zeng, J., 2012, Near-field deformation from the El Mayor–Cucapah earthquake revealed by differential LIDAR: Science, v. 335, no. 6069, p. 702-705.

Park, C. B., Miller, R. D., and Xia, J., 1999, Multichannel analysis of surface waves: Geophysics, v. 64, no. 3, p. 800-808.

Phelps, G., Graymer, R., Jachens, R., Ponce, D., Simpson, R., and Wentworth, C., 2008, Three-dimensional geologic map of the Hayward fault zone, San Francisco Bay region, California: US Geol. Surv. Scientific Invest. Map, v. 3045, p. 35.

Ponce, D. A., Burgmann, R., Graymer, R. W., Lienkaemper, J. J., Moore, D. E., and Schwartz, D. P., 2003, Proceedings of the Hayward Fault Workshop, Eastern San Francisco Bay Area, California, September 19-20, 2003, 2331-1258.

Rabruch-Hall, D. H., 1969, Areal and engineering geology of the Oakland East quadrangle, California.

Radbruch-Hall, D. H., 1974, Map showing recently active breaks along the Hayward fault zone and the southern part of the Calaveras fault zone, California.

Rubin, R. S., 2011, Ashland Fault, Alameda County, California. FER-255.

Shi, B., and Brune, J. N., 2005, Characteristics of near-fault ground motions by dynamic thrust faulting: two-dimensional lattice particle approaches: Bulletin of the Seismological Society of America, v. 95, no. 6, p. 2525-2533.

Simpson, R., Lienkaemper, J., and Galehouse, J., 2001, Variations in creep rate along the Hayward Fault, California, interpreted as changes in depth of creep: Geophys. Res. Lett, v. 28, no. 11, p. 2269-2272.

Smith, T. C., 1980, Hayward fault (Oakland segment).

Somerville, P., Saikia, C., Wald, D., and Graves, R., 1996, Implications of the Northridge earthquake for strong ground motions from thrust faults: Bulletin of the Seismological Society of America, v. 86, no. 1B, p. S115-S125.

Teran, O., Fletcher, J., Rockwell, T., Hudnut, K., Oskin, M., Akciz, S., Elliott, A., Gold, P., Liu, J., and Manjarrez, U., Structural Controls on the Surface Rupture Associated with the Mw7. 2 El Mayor-Cucapah Earthquake of 4 April 2010: A Comparative Analysis of Scarp Array Kinematics, Orientation, Lithology and Width, *in* Proceedings AGU Fall Meeting Abstracts2011, Volume 1, p. 2348.

US Geological Survey (USGS), 2006, U.S. Geological Survey Topographic LiDAR: Alameda County.

US Geological Survey (USGS), and California Geological Survey (CGS), 2006, Quaternary fault and fold database for the United States, accessed Aug 18, 2015, http//earthquakes.usgs.gov/regional/qfaults/.

Valensise, G., and Ward, S. N., 1991, Long-term uplift of the Santa Cruz coastline in response to repeated earthquakes along the San Andreas fault: Bulletin of the Seismological Society of America, v. 81, no. 5, p. 1694-1704.

Wei, S., Fielding, E., Leprince, S., Sladen, A., Avouac, J.-P., Helmberger, D., Hauksson, E., Chu, R., Simons, M., and Hudnut, K., 2011, Superficial simplicity of the 2010 El Mayor-Cucapah earthquake of Baja California in Mexico: Nature Geoscience, v. 4, no. 9, p. 615-618.

William Lettis & Associates, 1996, Fault trenching and characterization for a splay of the Ashland fault system in San Lorenzo, California.

Williams, P. L., 1998, Hayward fault slip vector and rate constraints at Berkeley: reinterpretations of EB landforms and tectonic hazards, The University.

Witter, R. C., Knudsen, K. L., Sowers, J. M., Wentworth, C. M., Koehler, R. D., Randolph, C. E., Brooks, S. K., and Gans, K. D., 2006, Maps of Quaternary deposits and liquefaction susceptibility in the central San Francisco Bay region, California: Geological Survey (US), 2331-1258.

10.0 FIGURES

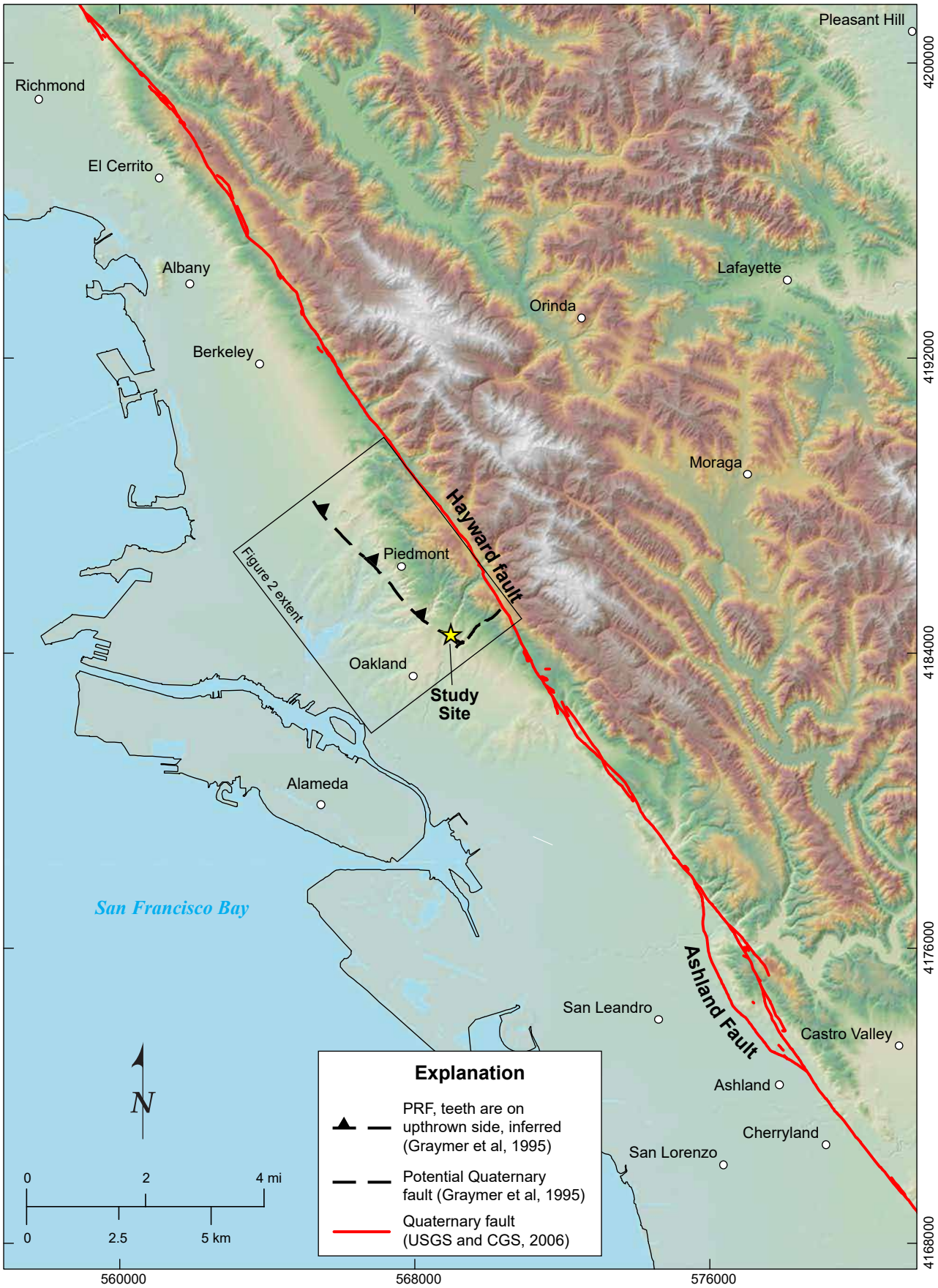

Figure 1. Shaded Relief Map of High Topography West of the Hayward fault.

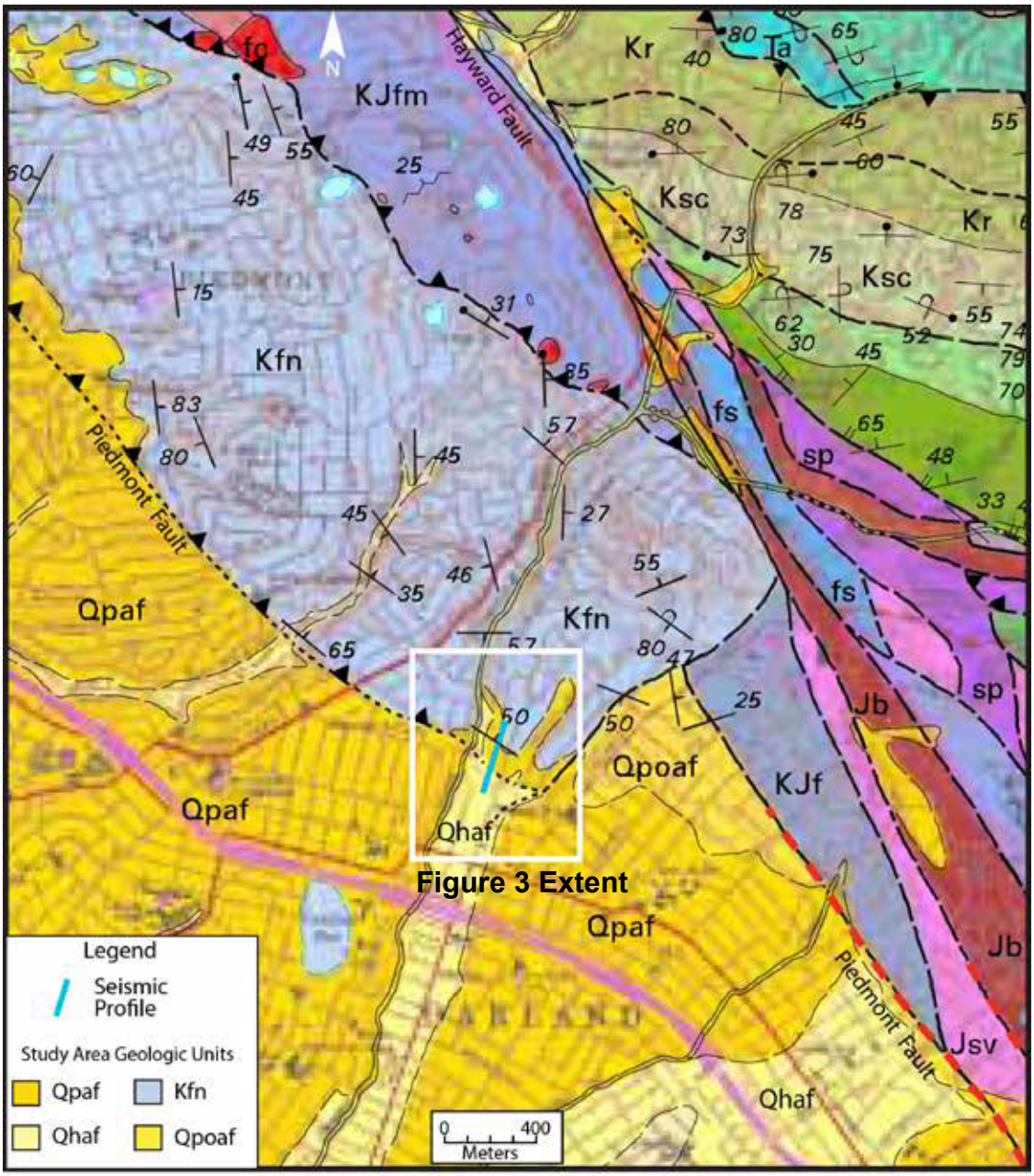

Figure 2. Geologic Map of the Study Region (Graymer et al., 1995)

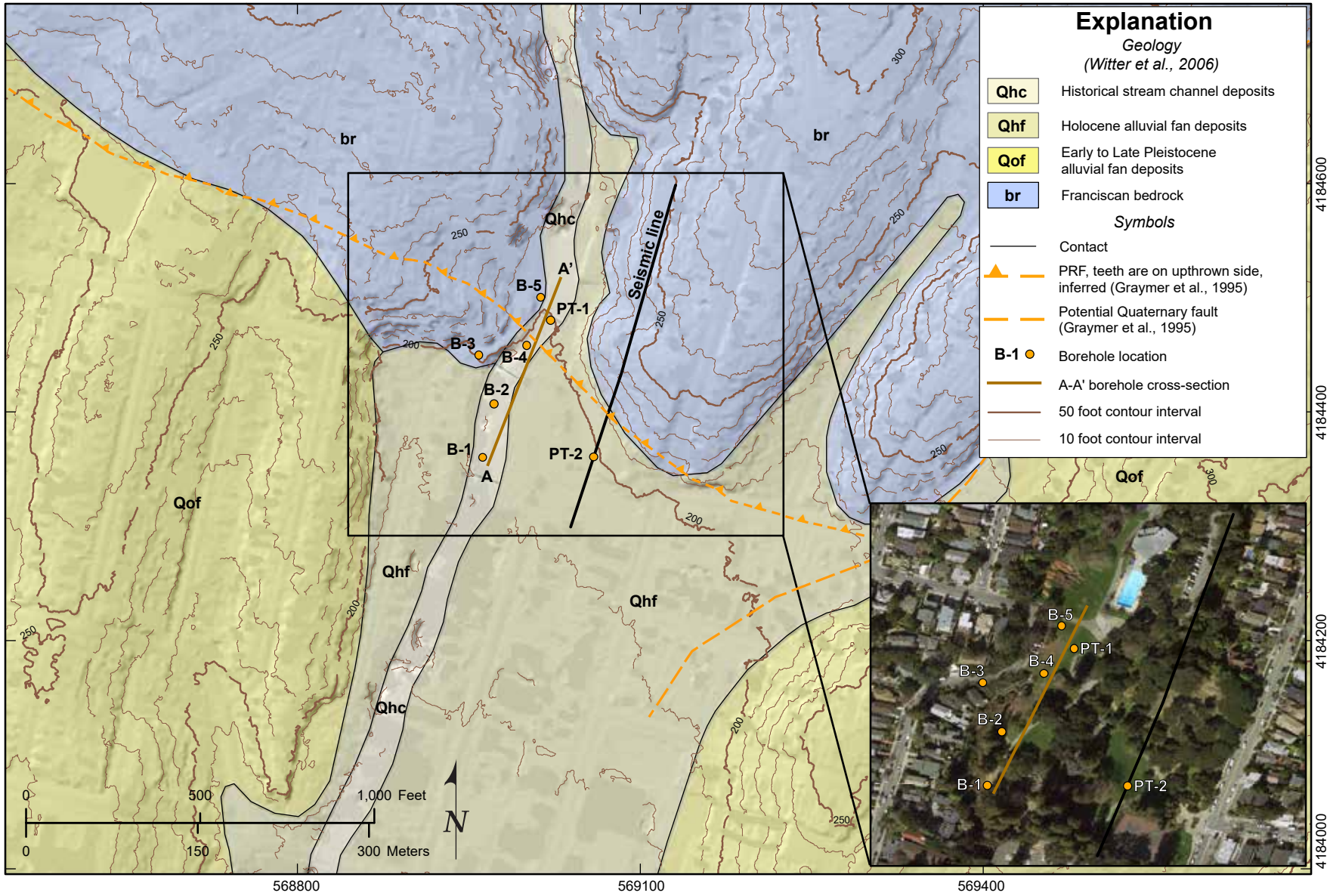

Figure 3. Quaternary Geology of Study Area Showing Data Collection Locations

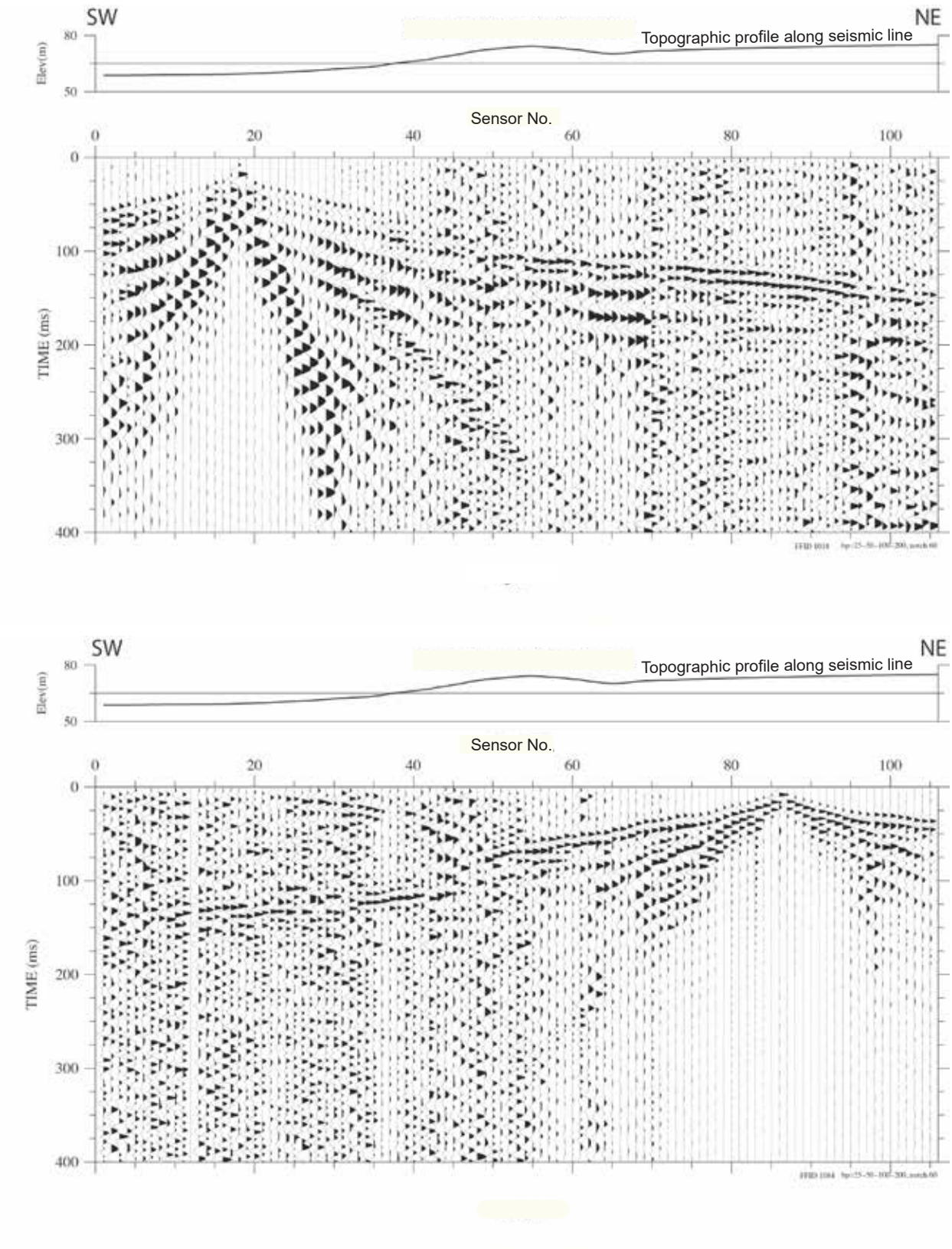

Figure 4. Example P-wave Shot Gathers

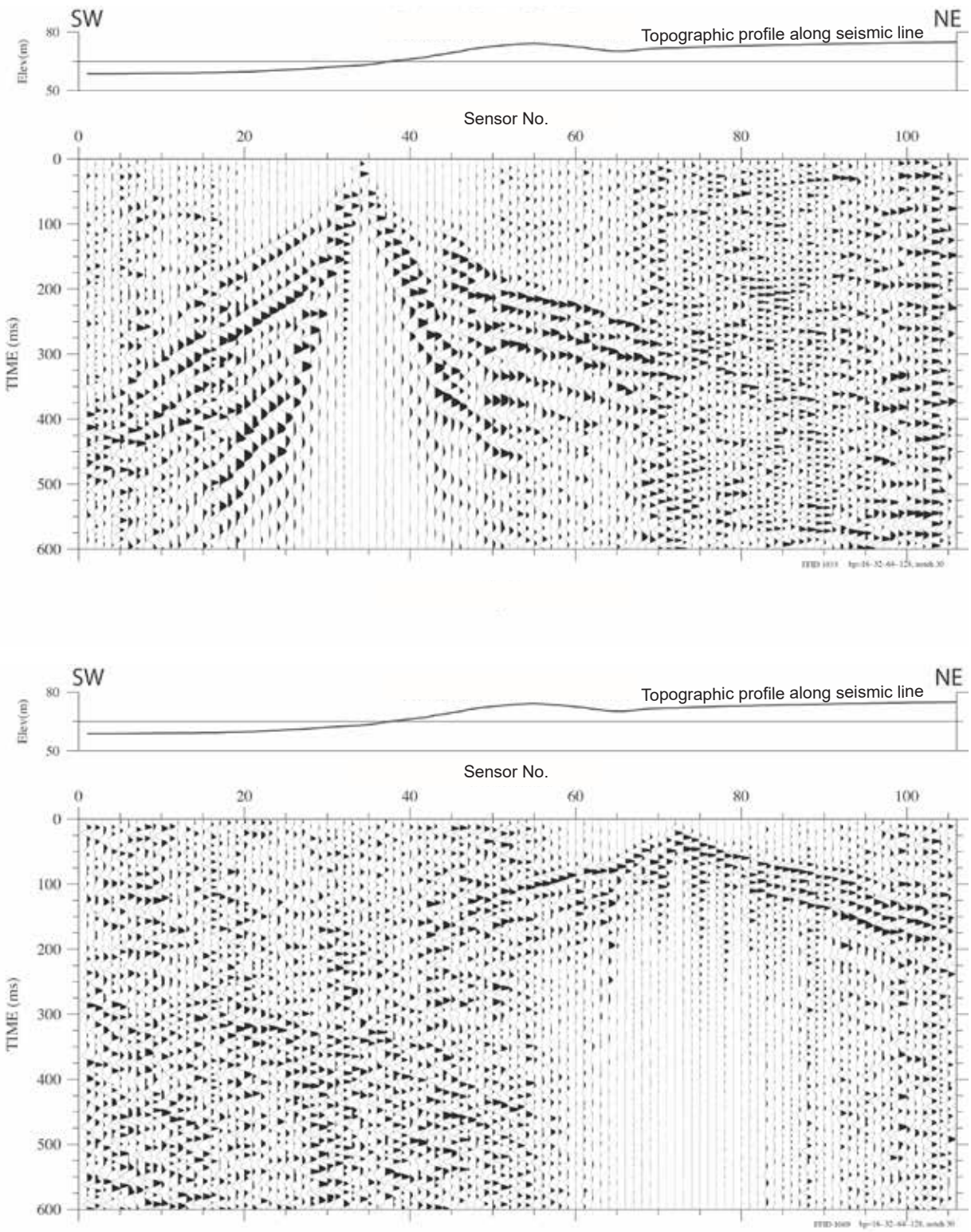

Figure 5. Example S-wave Shot Gathers

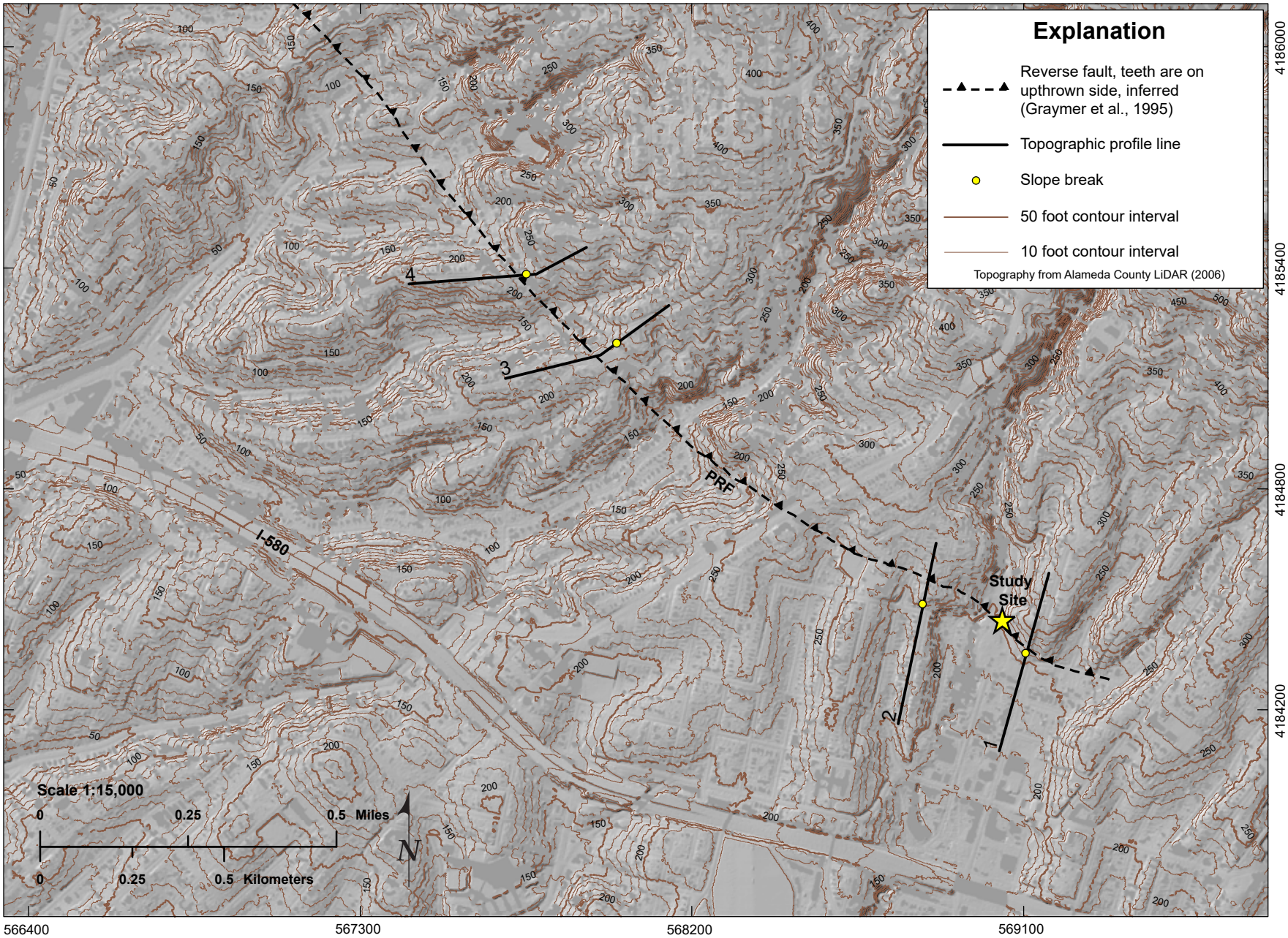

Figure 6. Shaded Relief Map of Piedmot Reverse Fault Showing Topographic Profile Locations

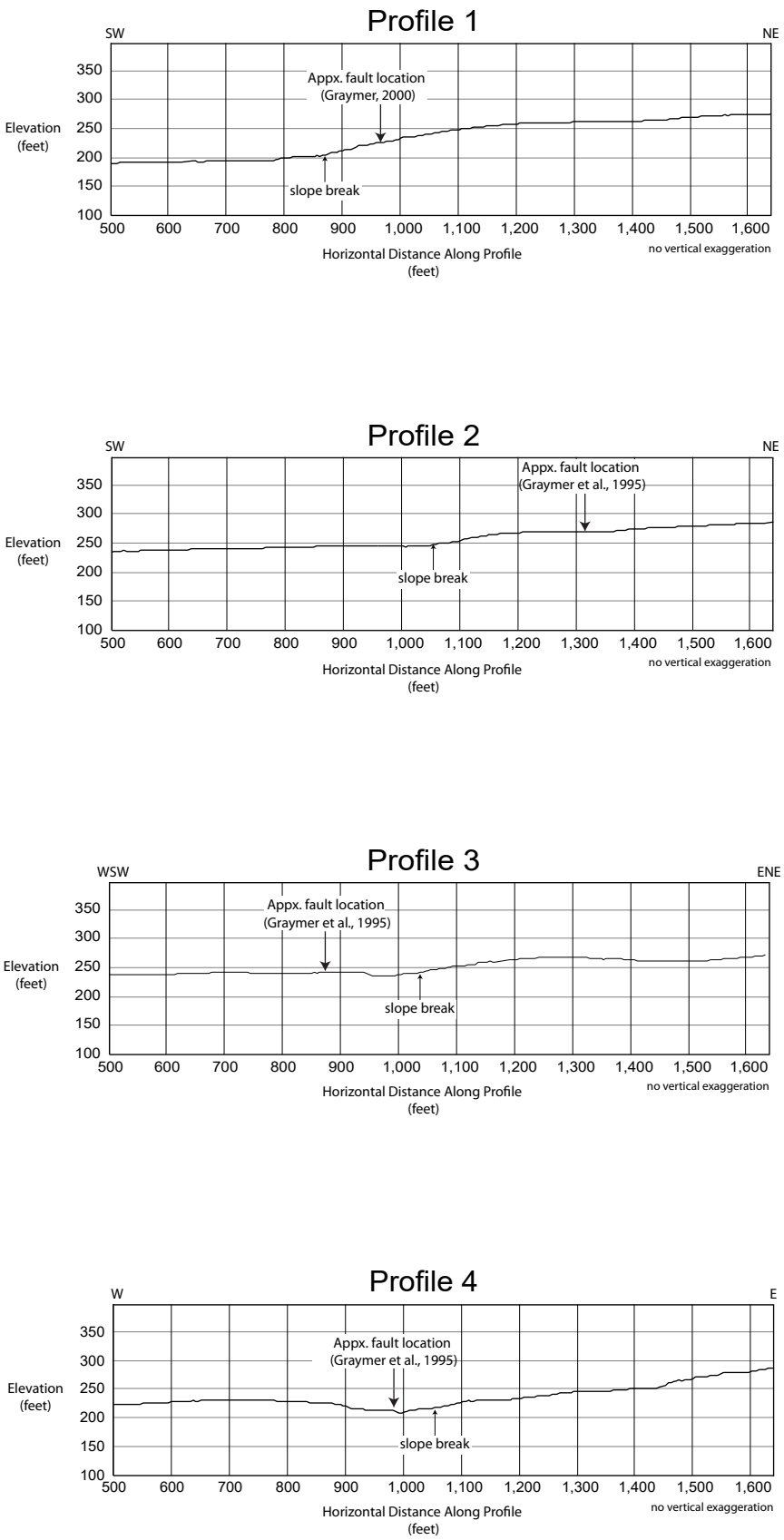

Figure 7. Topographic Profiles Across the Piedmont Reverse Fault

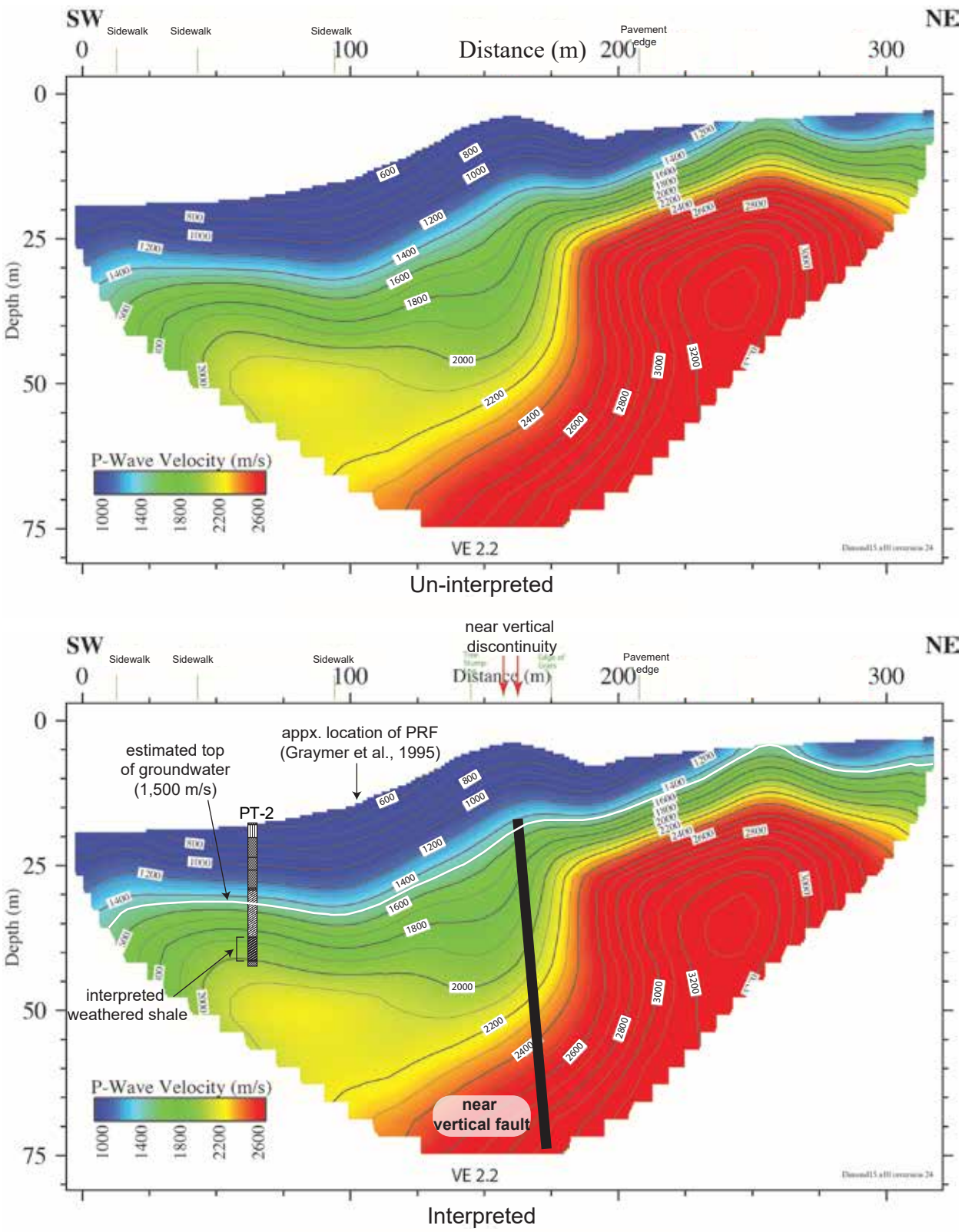

Figure 8. P-wave Refraction Tomography Velocity Model Cross-section, Un-interpreted (Top) and Interpreted (Bottom)

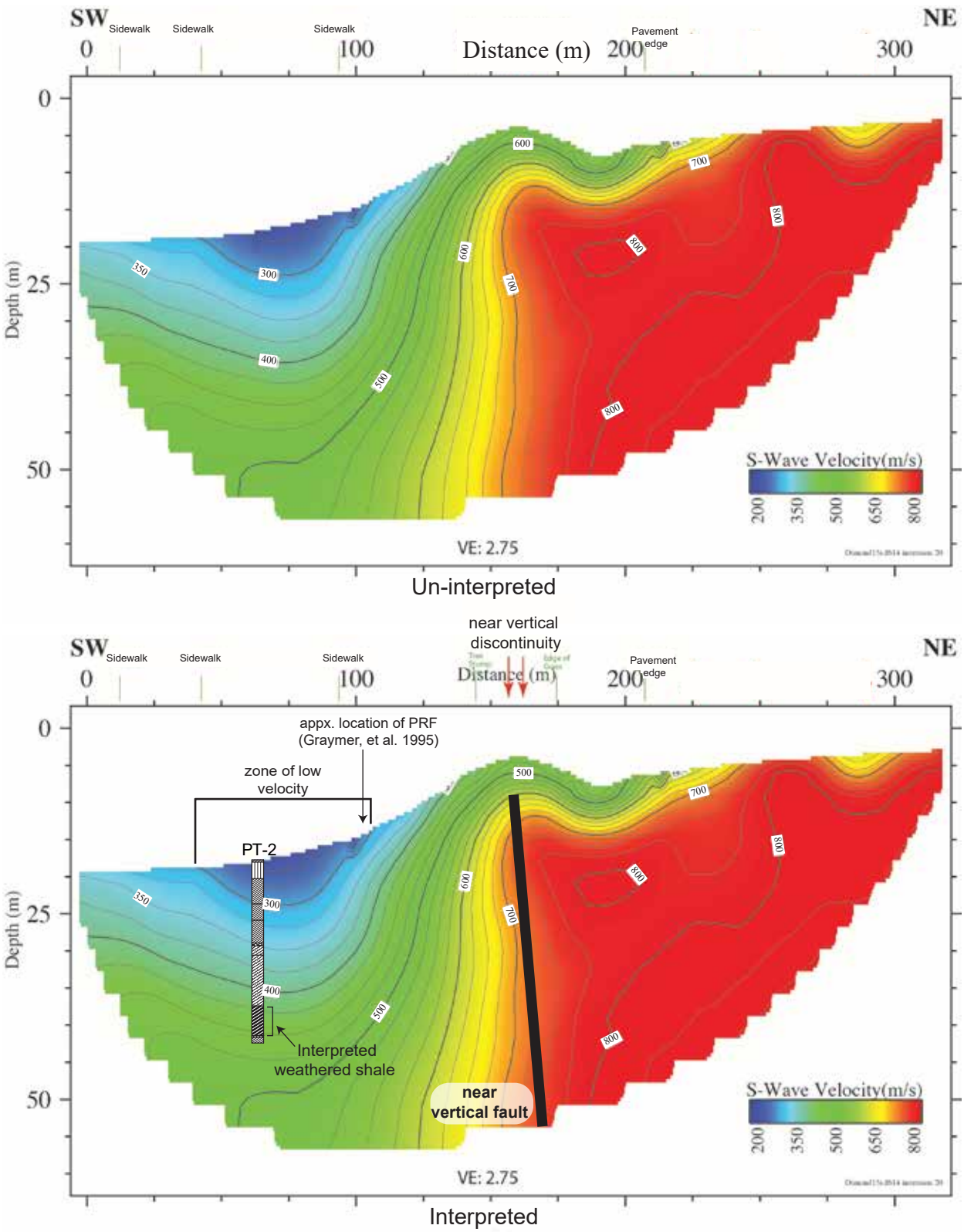

Figure 9. S-wave Refraction Tomography Velocity Model Cross-section, Un-interpreted (Top) and Interpreted (Bottom)

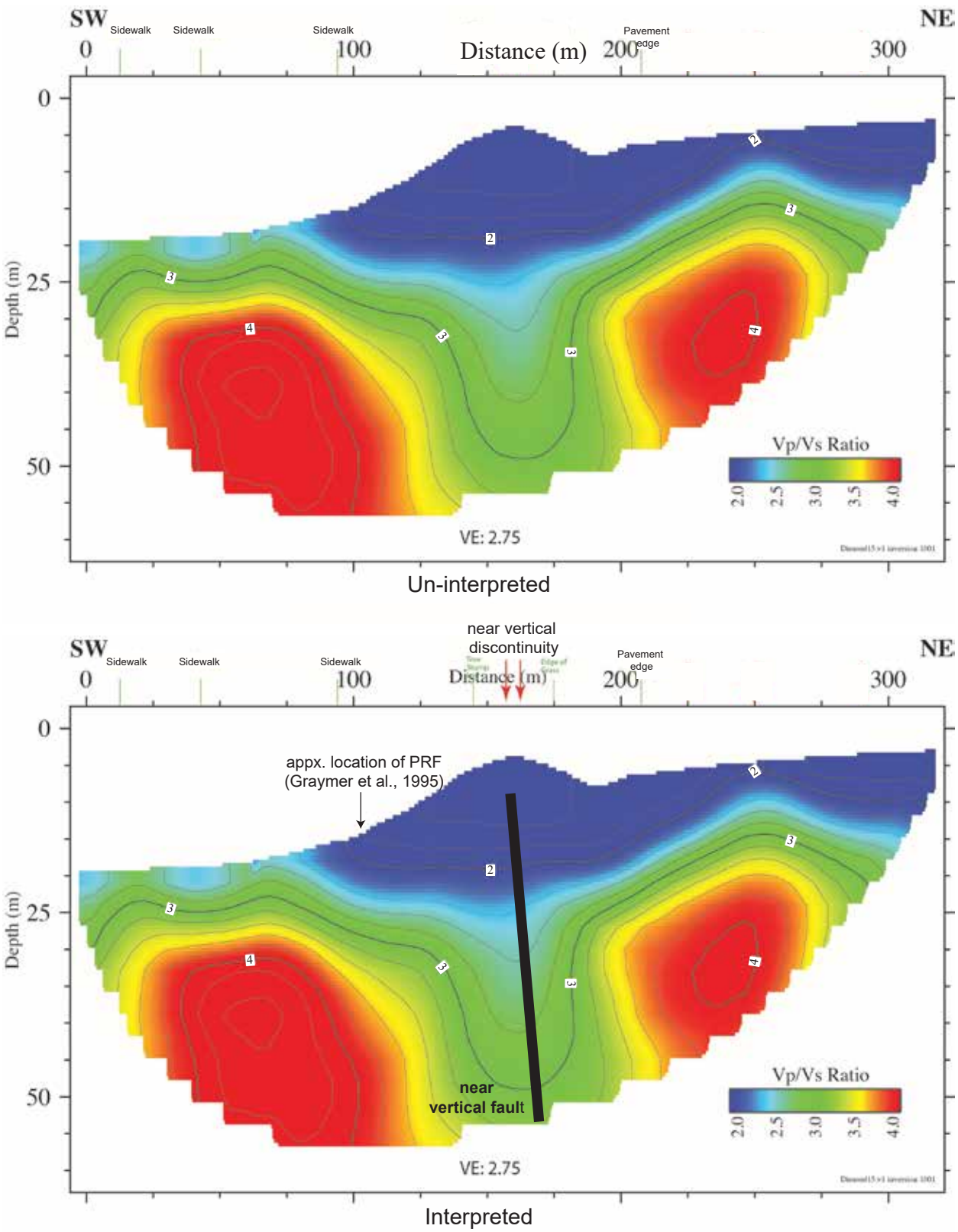

Figure 10. Vp/Vs Ratio Model Cross-section, Un-interpreted (Top) and Interpreted (Bottom)

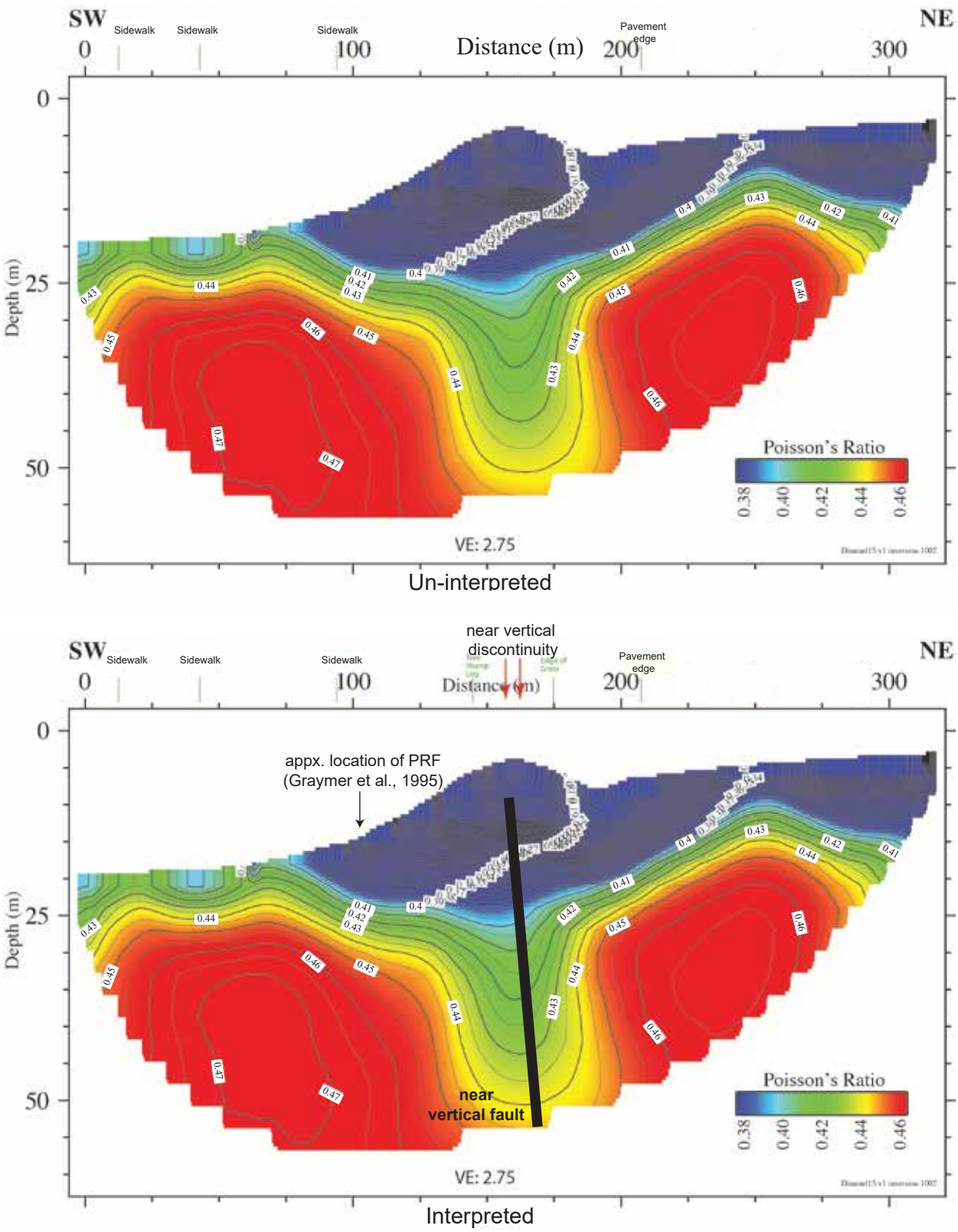

Figure 11. Poisson's Ratio Model Cross-section, Un-interpreted (Top) and Interpreted (Bottom)

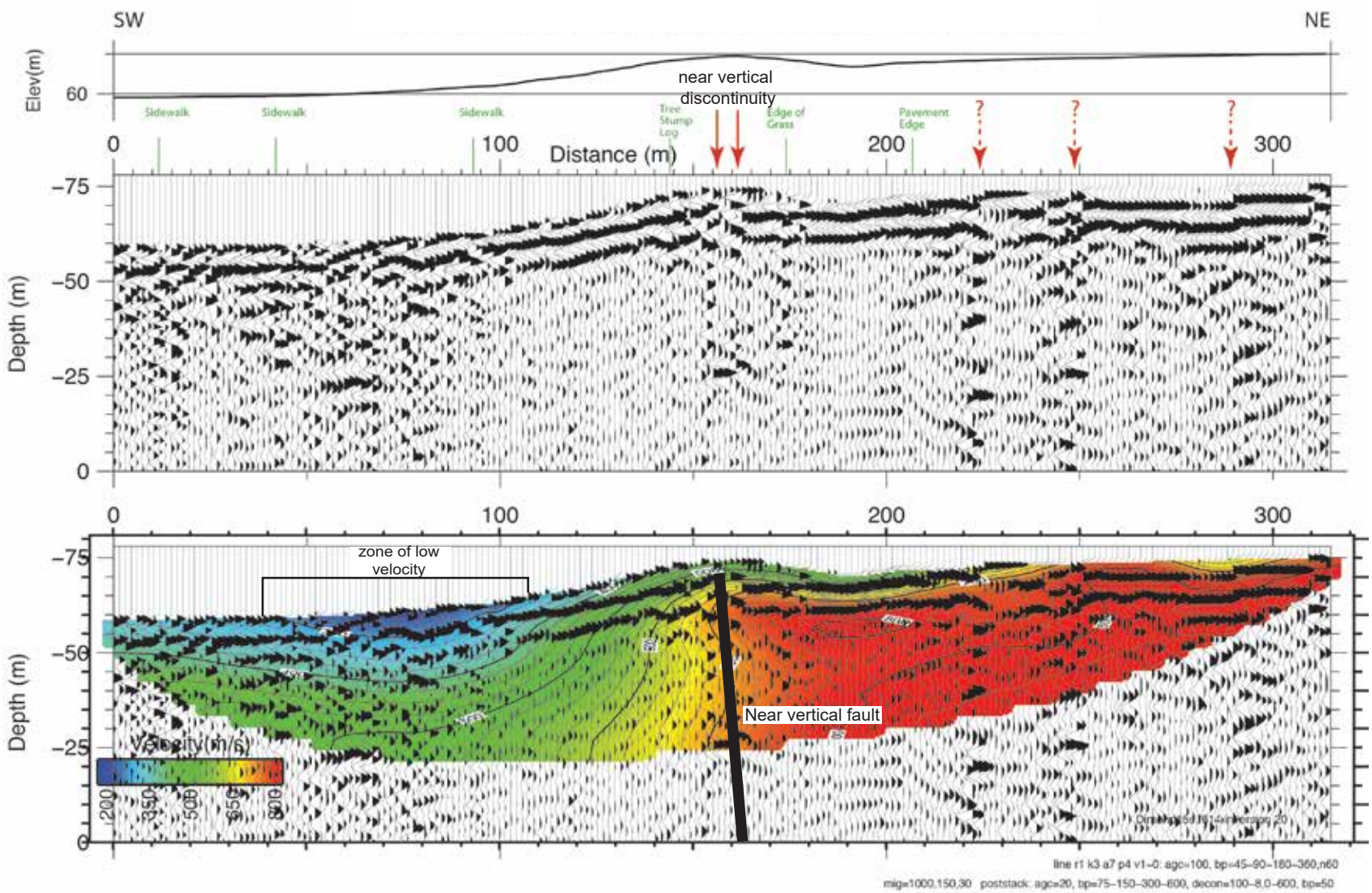

Figure 12. Seismic Reflection Stack Using P-wave Data

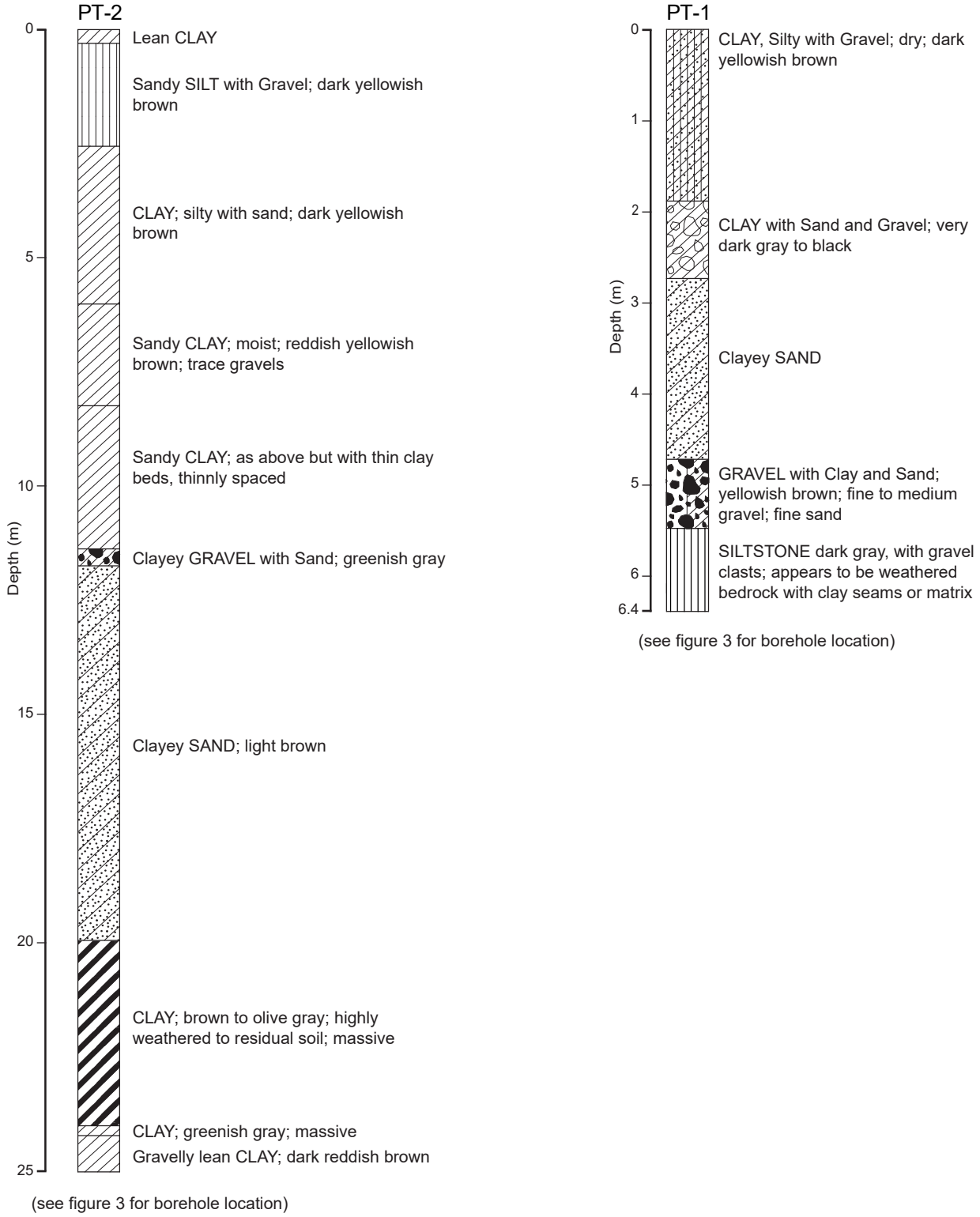

Figure 13. Summary Borehole Logs, PT-1 and PT-2

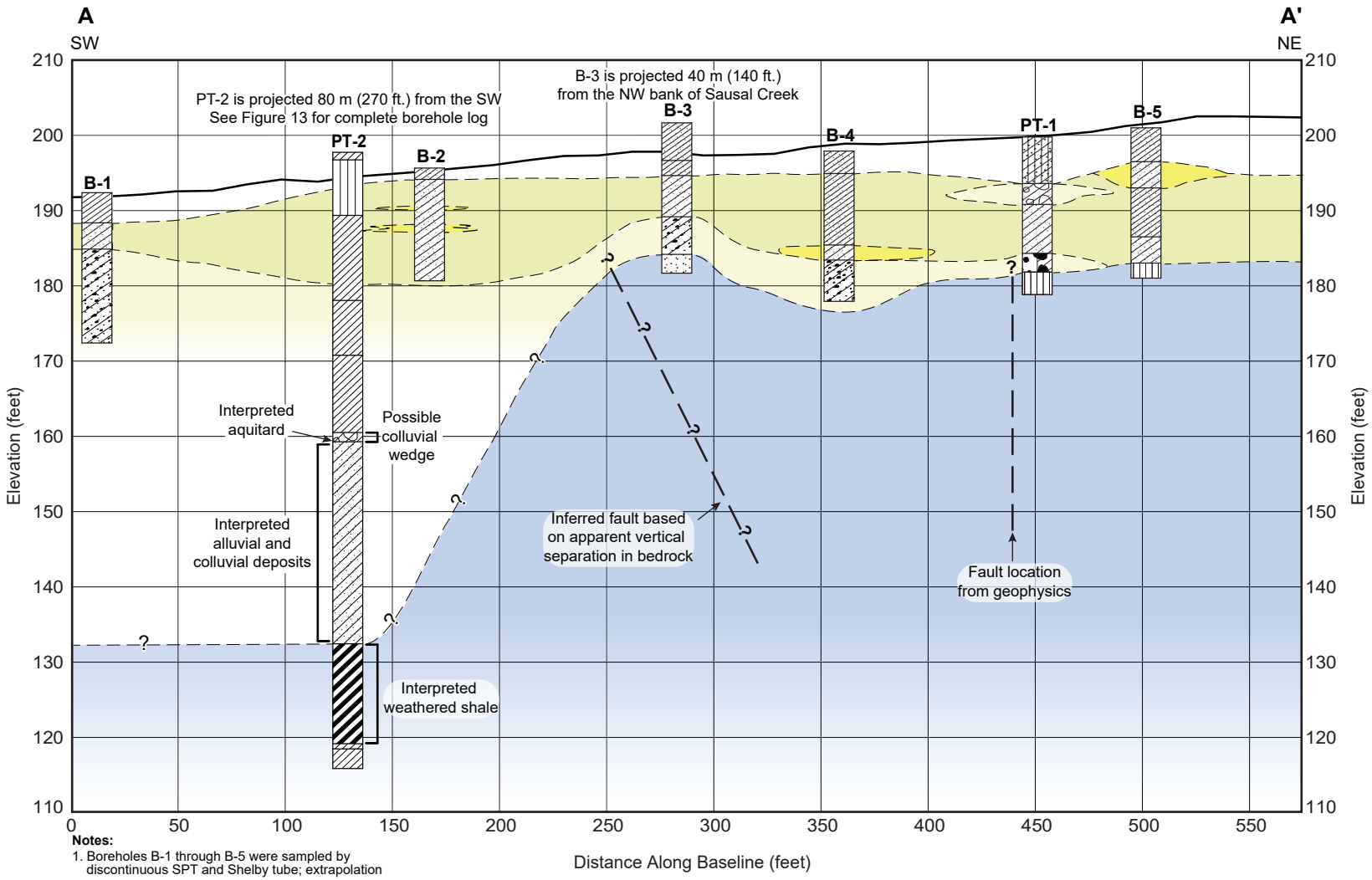

Notes:

1. Boreholes B-1 through B-5 were sampled by discontinuous SPT and Shelby tube; extrapolation of the lithologic data were done to illustrate stratigraphy.
2. vertical exaggeration = 3.5

Explanation

Borehole Symbols

- Silt
- Clay
- Clayey sand
- Sandy clay
- Clay, silty with gravel
- Clayey gravel
- Clay with sand and gravel
- Gravel with clay and sand
- Sandstone
- Siltstone

Weathered bedrock

Geology

Quaternary

- Fill
- Colluvium interfingered with overbank deposits
- Sausal Creek Channel deposits
- Sausal Creek overbank deposits

Franciscan

- Bedrock

Symbols

- Inferred contact
- Queried contact
- Queried fault
- Inferred fault

Figure 14. Borehole Cross-section A-A'

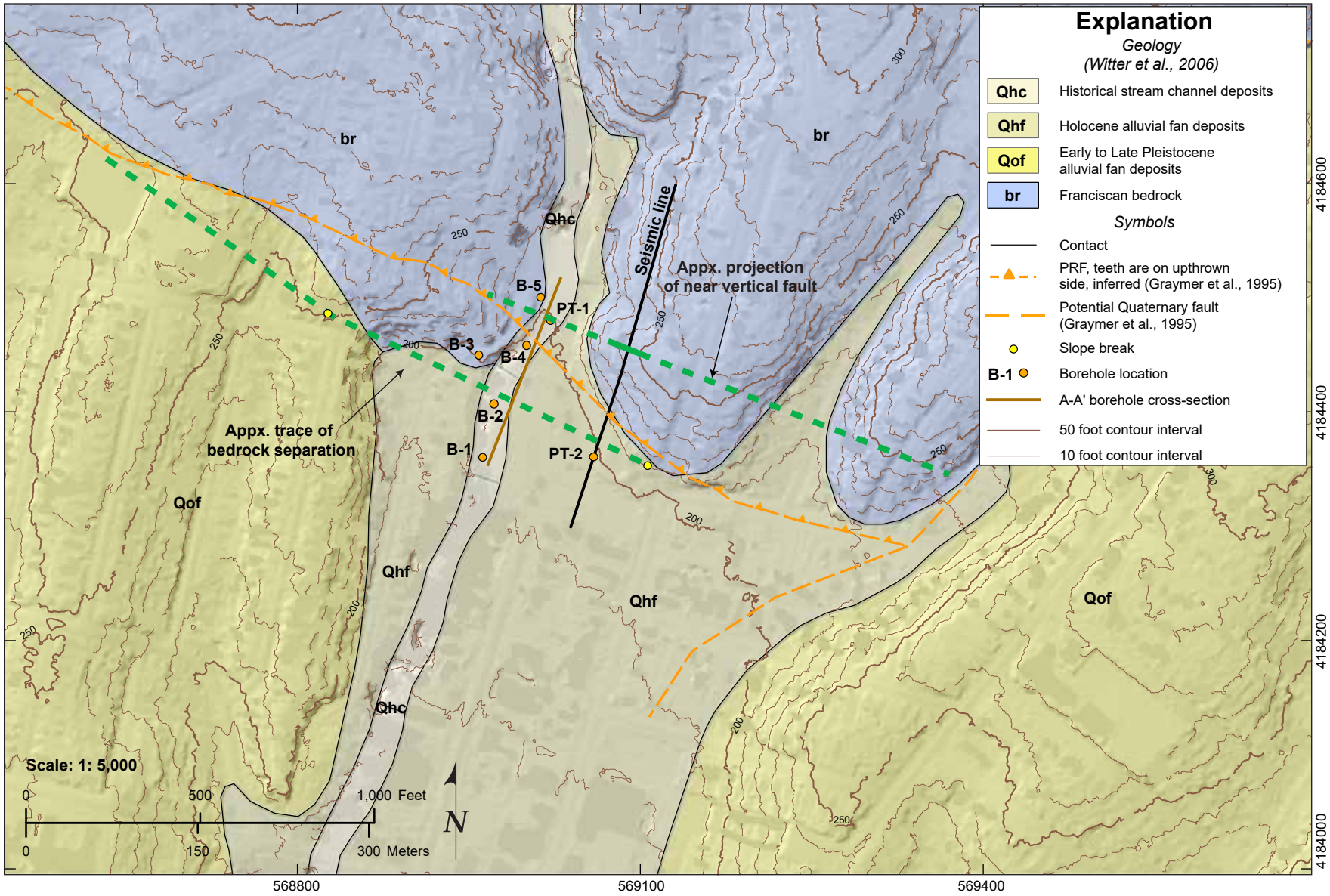

Figure 15. Interpreted location of Piedmont Reverse Fault, Constrained from Geophysics and Borehole Data

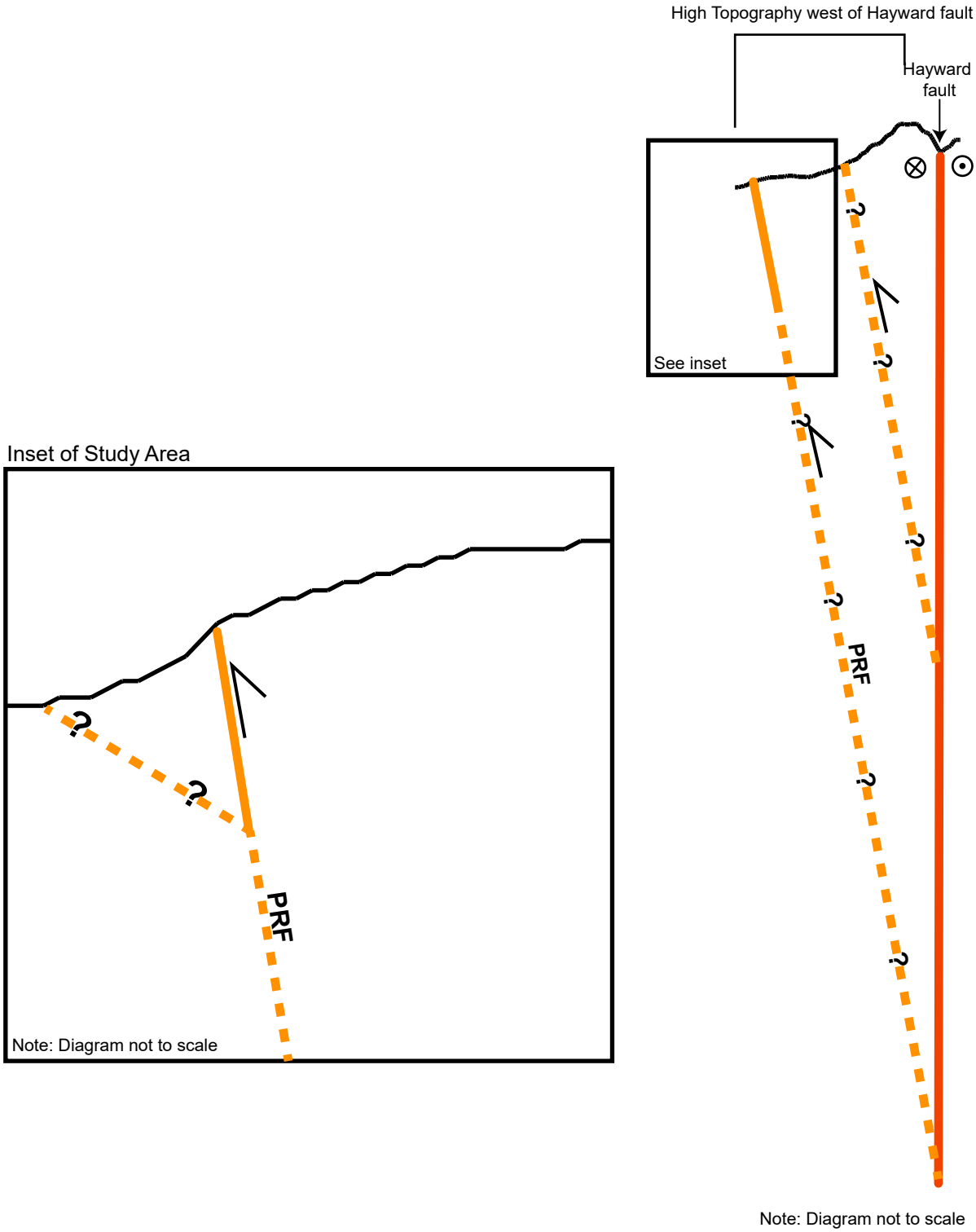

Figure 16. Conceptual Model of Piedmont Reverse Fault Connection to Hayward Fault

APPENDIX A

Borehole logs from Sausal Creek Restoration Project in Dimond Canyon Park Oakland, California

CLASSIFICATION AND MATERIAL SYMBOLS

MAJOR DIVISIONS PER ASTM D2488-06			MAJOR GROUP NAMES AND MATERIAL SYMBOLS	
COARSE-GRAINED SOILS More than 50% retained on the No. 200 sieve	GRAVELS MORE THAN 50% OF COARSE FRACTION RETAINED ON NO. 4 SIEVE	Clean gravels less than 5% fines	GW	Well-Graded GRAVEL
			GP	Poorly Graded GRAVEL
		Gravels with more than 12% fines	GM	SILTY GRAVEL
			GC	CLAYEY GRAVEL
	SANDS MORE THAN 50% OF COARSE FRACTION PASSING NO. 4 SIEVE	Clean sand less than 5% fines	SW	Well-Graded SAND
			SP	Poorly Graded SAND
		Sands with more than 12% fines	SM	SILTY SAND
			SC	CLAYEY SAND
FINE-GRAINED SOILS 50% or more passes the No. 200 sieve	SILTS AND CLAYS Liquid Limit Less than 50%		ML	SILT
			CL	Lean CLAY
			OL	ORGANIC SILT
	SILTS AND CLAYS Liquid Limit Greater than 50%		MH	Elastic SILT
			CH	Fat CLAY
			OH	ORGANIC CLAY
HIGHLY ORGANIC SOILS			PT	Peat or Highly Organic Soils

Notes:
Classification of soils on the boring logs is in general accordance with ASTM D2488, or D2487 if appropriate laboratory data are available.
The geologic formation is noted in bold font at the top of interpreted interval on the boring logs.

OTHER MATERIAL SYMBOLS

- Debris or Mixed Fill
- Pavement with Aggregate Base

SAMPLER TYPE

- SPT (Driven) 1-3/8" ID 2" OD
- Modified California (Driven) 2-3/8" ID 3" OD
- Modified California (Driven) 1-7/8" ID 2-1/2" OD
- Shelby Tube (Pushed) 2-7/8" ID 3" OD
- Pitcher Barrel (Rotary-cut) 2-7/8" ID
- Osterberg (Piston) 2-7/8" ID
- 101 Geobarrel (Rotary-cut) 2-7/8" ID
- Rock Core (Rotary-cut) See log for size
- Vibracore (Vibrated) See log for size
- Push-core (Pushed) See log for size
- Collected from Auger
- Other See log for details

Note: Refer to text of report for additional details or other sampler types.

BLOW COUNT

Number of blows required to drive sampler each of three 6-in. intervals, as measured in the field (uncorrected). An SPT hammer (140 lb., falling 30-in.) was used unless otherwise noted on the boring log. For example:

Blow Count	Description
5 7 8	5, 7, and 8 blows for first, second, and third interval, respectively.
35 50/3"	35 blows for the first interval. 50 blows for the first 3 inches of the second interval. Lack of third value implies that driving was stopped 3 inches into the second interval.
WOH WOH 5	"WOH" indicates that the weight of the hammer was sufficient to advance the sampler over the first two intervals. 5 blows were required to advance the sampler over the third interval.

N-VALUE

The N-Value represents the blowcount for the last 12 inches of the sample drive if three 6-inch intervals were driven. N-value presented is independant of impact energy. If 50 hammer blows were insufficient to drive through either the second or the third interval, the total number of blows and total length driven are reported (excluding the first interval). "ref" (refusal) indicates that 50 blows were insufficient to drive through the first 6-inch interval.

Parenthesis indicate that an approximate correction has been applied for non-SPT drive samplers. For example, a factor of 0.63 is commonly used to adjust blow counts obtained using a 3-inch outside diameter modified California sampler to correspond to Standard Peneteration Test.

UNDRAINED SHEAR STRENGTH

A value of undrained shear strength is reported. The value is followed by a letter code indicating the type of test that was performed, as follows:

U - Unconfined Compression
Q - Unconsolidated Undrained Triaxial
T - Torvane
P - Pocket Penetrometer
M - Miniature Vane
F - Field Vane
R - R-value

OTHER TESTS

Field or laboratory tests without a dedicated column on the boring log are reported in the Other Tests column. A letter code is used to indicate the type of test. For certain tests, a value representing the test result is also provided. Typical letter codes are as follows. Additional codes may be used. Refer to the report text and the laboratory testing results for additional information.

k - Permeability (cm/s)
Consol - Consolidation
Gs - Specific Gravity
MA - Particle Size Analysis
EI - Expansion Index
OVM - Organic Vapor Meter

WATER LEVEL SYMBOLS

- Initial water level
- Final water level
- Seepage encountered

INCREASING MOISTURE CONTENT

Dry
Moist
Wet

CONSISTENCY OF COHESIVE SOIL

CONSISTENCY	UNDRAINED SHEAR STRENGTH (KIPS PER SQUARE FOOT)
Very Soft	< 0.25
Soft	0.25 to 0.50
Medium Stiff	0.50 to 1.0
Stiff	1.0 to 2.0
Very Stiff	2.0 to 4.0
Hard	> 4.0

Note: In absence of test data, consistency has been estimated based on manual observation.

APPARENT DENSITY OF COHESIONLESS SOIL

APPARENT DENSITY	N-VALUE
Very Loose	0 to 4
Loose	5 to 9
Medium Dense	10 to 29
Dense	30 to 49
Very Dense	> 49

TERMS AND SYMBOLS USED ON BORING LOGS

PLATE A-1

MATERIAL SYMBOLS

	Sandstone
	Siltstone
	Claystone
	Basalt
	Bolders and Cobbles
	Other (refer to boring log)

Note: Composite or additional symbols may be shown on boring log. Refer to material description on boring log.

GRAIN SIZE FOR CRYSTALLINE IGNEOUS AND METAMORPHIC ROCK

DESCRIPTION	AVERAGE CRYSTAL DIAMETER
Very Coarse Grained or Pegmatic	Greater of equal to 3/8 inch
Coarse-Grained	3/16 to 3/8 inch
Medium-Grained	1/32 to 3/16 inch
Fine-Grained	1/250 to 1/32 inch
Aphanitic	Less than 1/250 inch

WEATHERING OF INTACT ROCK

DESCRIPTION	CHARACTERISTICS
Fresh	No discoloration, not oxidized.
Slightly Weathered	Discoloraton or oxidation is limited to surface of, or short distance from fractures; some feldspar crystals are dull.
Moderately Weathered	Discoloration or oxidation extends from fractures usually throughout; Fe-Mg minerals are "rusty", feldspar crystals are "clowdy".
Intensely Weathered	Discoloration or oxidation throughout; all feldspars and Fe-Mg minerals are altered to clay to some extent; or chemical alteration produces in situ disaggregation, see grain boundary conditions.
Decomposed	Discolored or oxidized throughout, but resistant minerals such as quartz may be unaltered; all feldspars and Fe-Mg minerals are completely altered to clay.

BEDDING SPACING

DESCRIPTION	THICKNESS/SPACING
Massive	Greater than 10 feet.
Very Thickly Bedded	3 to 10 feet.
Thickly Bedded	1 to 3 feet.
Moderately Bedded	4 inches to 1 foot.
Thinly Bedded	1 to 4 inches.
Very Thinly Bedded	1/4 to 1 inch.
Laminated	Less than 1/4 inch.

HARDNESS

DESCRIPTION	CRITERIA
Extremely Hard	Cannot be scratched with a pocket knife or sharp pick. Can only be chipped with repeated heavy hammer blows.
Very Hard	Cannot be scratched with a pocket knife or sharp pick. Breaks with repeated heavy hammer blows.
Hard	Can be scratched with a pocket knife or sharp pick with difficulty (heavy pressure). Breaks with heavy hammer blows.
Moderately Hard	Can be scratched with a pocket knife or sharp pick with light or moderate pressure. Core breaks with moderate hammer blows.
Moderately Soft	Can be grooved 1/6-inch deep with a pocket knife or sharp pick with moderate or heavy pressure. Breaks with light hammer blow or heavy manual pressure.
Soft	Can be grooved or gouged easily with a pocket knife or sharp pick with light pressure. Can be scratched with fingernail. Breaks with light to moderate manual pressure.
Very Soft	Can be readily indented, grooved or gouged with fingernail, or carved with a pocketknife. Breaks with light manual pressure.

FRACTURE DENSITY

DESCRIPTION	OBSERVED FRACTURE DENSITY
Unfractured	No fractures.
Very Slightly Fractured	Core lengths greater than 3 feet.
Slightly Fractured	Core lengths mostly from 1 to 3 feet.
Moderately Fractured	Core lengths mostly 4 inches to 1 foot.
Intensely Fractured	Core lengths mostly from 1 to 4 inches.
Very Intensely Fractured	Mostly chips and fragments.

TERMS AND SYMBOLS USED FOR ROCK

PLATE A-2

LOCATION: East of Sausal Creek

DEPTH, ft	MATERIAL SYMBOL	SAMPLER TYPE	BLOW COUNT OR PRESSURE, psi	N VALUE OR RQD%	RECOVERY	MATERIAL DESCRIPTION	DRY UNIT WEIGHT, pcf	WATER CONTENT, %	% PASSING #200 SIEVE	LIQUID LIMIT, %	PLASTICITY INDEX	UNDRAINED SHEAR STRENGTH, S_u, ksf	OTHER TESTS
			2 3 3	4	15/18"	Lean CLAY with SAND (CL): medium stiff, yellowish brown, dry to moist, medium plasiticity, fine to medium grained sand, asphalt debris, few rootlets (FILL)							
								14		30	16		
			4 4 4	5	13/18"								
5			3 3 5	5	16/18"	CLAYEY SAND (SC): loose, dark brown, dry to moist, fine sand, trace medium grained sand, low to medium plasticity fines	97	15	46				
			13 13 22	23	18/18"	CLAYEY SAND with GRAVEL (SC): medium dense, light yellowish brown, dry, fine to coarse grained sand, mostly fine to medium grained, fine to coarse gravel, mostly gravel less than 3/4" diameter, subrounded to subangular		5					
10													
			18 15 15	30	11/18"	- dense, increase gravels, angular gravel ranging from 1/2" to 1.5" diameter below 13.5' - wet below 14.2'							
15													
						- medium dense, interbedded with sandy clay							
			2 5 11	16	17/18"								
20													
						Boring end @ 20' NOTES: 1. Terms and symbols defined on Plate A-1.							

BORING DEPTH: 20.0 ft
BACKFILL: Grout
DEPTH TO WATER: 14.2 ft
FIELDWORK DATE: May 2, 2011
DRILLING METHOD: 4-in. dia. Solid Stem Auger

HAMMER TYPE: Automatic Trip
RIG TYPE: CME-55
DRILLED BY: Britton Exploration, Paul Britton
LOGGED BY: A Sperske
CHECKED BY:

LOG OF BORING NO. B-1
Sausal Creek Restoration Project
Oakland, California

FWI STANDARD LOG BETA02 G:\JOBDOCS\04.71110022 SAUSAL CREEK\EXPLORATIONS\BORINGS\SAUSALCREEK_20110517.GPJ OGEM_LIB_MARCH2011.GLB 5/18/11 07:14 p

LOCATION: East of Sausal Creek

DEPTH, ft	MATERIAL SYMBOL	SAMPLER TYPE	BLOW COUNT OR PRESSURE, psi	N VALUE OR RQD%	RECOVERY	MATERIAL DESCRIPTION	DRY UNIT WEIGHT, pcf	WATER CONTENT, %	% PASSING #200 SIEVE	LIQUID LIMIT, %	PLASTICITY INDEX	UNDRAINED SHEAR STRENGTH, S_u, ksf	OTHER TESTS
						SANDY Lean CLAY (CL): medium stiff, yellowish brown, dry, low to medium plasticity, fine grained sand, trace organics							
			2 2 2	3	12/18"	CLAYEY SAND (SC): loose, yellowish brown, dry to moist, fine to medium grained sand	85	16					
			3 4 4	5	15/18"	- few gravels up to 1/2" diameter, subangular			31				
5			4 5 6	7	13/18"	- increase fines content at 5.5'							
						- medium dense, light olive brown, moist, interbedded with gray clayey sand, medium plasticity, fine sand, few fine gravel below 7.5'							
			4 8 11	12	14/18"		102	22	46			1.3 P	
10													
			5 11 12	15	18/18"	- increasing gravel, subangular							
15													
						End boring @ 15' NOTES: 1. Terms and symbols defined on Plate A-1.							

BORING DEPTH: 15.0 ft
BACKFILL: Grout
DEPTH TO WATER: 14.0 ft
FIELDWORK DATE: May 2, 2011
DRILLING METHOD: 4-in. dia. Solid Stem Auger

HAMMER TYPE: Automatic Trip
RIG TYPE: CME-55
DRILLED BY: Britton Exploration, Paul Britton
LOGGED BY: A Sperske
CHECKED BY:

LOG OF BORING NO. B-2
Sausal Creek Restoration Project
Oakland, California

FWI STANDARD LOG BETA02 G:\JOBDOCS\04.71110022 SAUSAL CREEK\EXPLORATIONS\BORINGS\SAUSALCREEK_20110517.GPJ OGEM_LIB_MARCH2011.GLB 5/18/11 07:14 p

LOCATION: West of Sausal Creek

DEPTH, ft	MATERIAL SYMBOL	SAMPLER TYPE	BLOW COUNT OR PRESSURE, psi	N VALUE OR RQD%	RECOVERY	MATERIAL DESCRIPTION	DRY UNIT WEIGHT, pcf	WATER CONTENT, %	% PASSING #200 SIEVE	LIQUID LIMIT, %	PLASTICITY INDEX	UNDRAINED SHEAR STRENGTH, S_u, ksf	OTHER TESTS
			2 1 2	2	11/18"	Sandy Lean CLAY (CL): medium stiff, dark brown, moist, with light yellowish brown inclusions, medium plasticity, fine to medium grained sand, few gravels, up to 3/4" diameter, subangular		16					
			2 1 3	3	14/18"							0.8 P	
5			3 4 6	7	16/18"	- increase gravels, angular to subangular below 5.0'	114	13		28	10		
			7 8 3	7	14/18"	CLAYEY SAND (SC): loose, dark brown, moist, medium plasticity, fine to medium grained sand, gravels up to 2" diameter, mostly up to 3/4" diameter, angular to subangular			48				
10													
			13 15 12	18	13/18"	CLAYEY SAND with GRAVEL (SC): medium dense, dark brown, moist, fine to medium grained sand, medium plasticity, gravels up to 2" diameter, mostly up to 3/4" diameter, angular to subangular	120	10	35				
15													
				50/2"	2/18"	SANDSTONE: light gray, dry, moderate hard to hard, slightly to moderately weathered, fine grained							
20						Boring end @ 20' NOTES: 1. Terms and symbols defined on Plate A-1.							

BORING DEPTH: 20.0 ft
BACKFILL: Grout
DEPTH TO WATER: 14.5 ft
FIELDWORK DATE: May 2, 2011
DRILLING METHOD: 4-in. dia. Solid Stem Auger

HAMMER TYPE: Automatic Trip
RIG TYPE: CME-55
DRILLED BY: Britton Exploration, Paul Britton
LOGGED BY: A Sperske
CHECKED BY:

LOG OF BORING NO. B-3
Sausal Creek Restoration Project
Oakland, California

FWI STANDARD LOG BETA02 G:\JOBDOCS\04.71110022 SAUSAL CREEK\EXPLORATIONS\BORINGS\SAUSALCREEK_20110517.GPJ OGEM_LIB_MARCH2011.GLB 5/18/11 07:14 p

LOCATION: East of Sausal Creek

DEPTH, ft	MATERIAL SYMBOL	SAMPLER TYPE	BLOW COUNT OR PRESSURE, psi	N VALUE OR RQD%	RECOVERY	MATERIAL DESCRIPTION	DRY UNIT WEIGHT, pcf	WATER CONTENT, %	% PASSING #200 SIEVE	LIQUID LIMIT, %	PLASTICITY INDEX	UNDRAINED SHEAR STRENGTH, S_u, ksf	OTHER TESTS
			5 5 6	7	12/18"	SANDY Lean CLAY with GRAVEL (CL): medium stiff, dark brown, moist, medium plasticity, fine to medium grained sand, gravel up to 2.5" diameter, mostly fine gravels, angular to subanglular	103	12					
			2 3 4	5	13/18"	SANDY Lean CLAY (CL): medium stiff to stiff, yellowish brown, moist, medium plasticity, mostly fine sand, trace coarse sand and fine gravel, trace organics						1.2 P	
5			2 3 5	5	12/18"	- light yellowish brown, medium stiff below 5.0'	104	21	53			0.6 P	
10			5 7 9	10	13/18"	- stiff, fine sand below 8.5'						1.5 P	
			7 17 19	23	18/18"	CLAYEY SAND (SC): medium dense, light olive brown, wet, with gray inclusions, fine to medium grained sand							
15						CLAYEY SAND with GRAVEL (SC): medium dense, yellowish brown, wet, fine to coarse grained sand, fine to coarse gravels, up to 2" diameter, subrounded to subangular							
20			17 10 10	20	5/18"	- 1.5" clay lens at 18.7'							

Boring end @ 20'
NOTES:
1. Terms and symbols defined on Plate A-1.

BORING DEPTH: 20.0 ft
BACKFILL: Grout
DEPTH TO WATER: 13.5 ft
FIELDWORK DATE: May 2, 2011
DRILLING METHOD: 4-in. dia. Solid Stem Auger

HAMMER TYPE: Automatic Trip
RIG TYPE: CME-55
DRILLED BY: Britton Exploration, Paul Britton
LOGGED BY: A Sperske
CHECKED BY:

LOG OF BORING NO. B-4
Sausal Creek Restoration Project
Oakland, California

FWI STANDARD LOG BETA02 G:\JOBDOCS\04.71110022 SAUSAL CREEK\EXPLORATIONS\BORINGS\SAUSALCREEK_20110517.GPJ OGEM_LIB_MARCH2011.GLB 5/18/11 07:14 p

LOCATION: East of Sausal Creek

DEPTH, ft	MATERIAL SYMBOL	SAMPLER TYPE	BLOW COUNT OR PRESSURE, psi	N VALUE OR RQD%	RECOVERY	MATERIAL DESCRIPTION	DRY UNIT WEIGHT, pcf	WATER CONTENT, %	% PASSING #200 SIEVE	LIQUID LIMIT, %	PLASTICITY INDEX	UNDRAINED SHEAR STRENGTH, S_u, ksf	OTHER TESTS
			12 14 15	19	15/18"	SANDY Lean CLAY (CL): stiff to very stiff, dark brown, moist, medium plasticity, fine to coarse grained sand, mostly fine to medium grained, trace roots (FILL)							
						- brick debris at 2.0'	119	11				4.0 P	
						- medium stiff							
			5 6 5	7	16/18"								
						CLAYEY SAND (SC): loose, yellowish brown, moist, medium plasticity, mostly fine grained sand, gravel up to 2.5" diameter, internsely weathered sandstone inclusions, trace organics				30	15		
5			4 4 4	5	12/18"		111	14	43			1.3 P	
						SANDY Lean CLAY (CL): medium stiff, dark brownish gray, moist, medium plasticity, few fine gravels, subangular							
			2 3 3	4	18/18"								
10												0.5 P	
						- olive brown interbedded with gray, wet, trace roots below 13.5'							
			3 6 12	12	18/18"								
15						CLAYEY SAND (SC): medium dense, yellowish brown, wet, fine to coarse grained sand, few fine gravels, subangular							
						SILTSTONE: decomposed to intensely weathered, brownish gray, dry, moderately soft, sandstone clasts, fine grained							
			11 21 46	67	8/18"								
20						Boring end @ 20' NOTES: 1. Terms and symbols defined on Plate A-1.							

BORING DEPTH: 20.0 ft
BACKFILL: Grout
DEPTH TO WATER: 13.5 ft
FIELDWORK DATE: May 2, 2011
DRILLING METHOD: 4-in. dia. Solid Stem Auger

HAMMER TYPE: Automatic Trip
RIG TYPE: CME-55
DRILLED BY: Britton Exploration, Paul Britton
LOGGED BY: A Sperske
CHECKED BY:

FWI STANDARD LOG BETA02 G:\JOBDOCS\04.71110022 SAUSAL CREEK\EXPLORATIONS\BORINGS\SAUSALCREEK_20110517.GPJ OGEM_LIB_MARCH2011.GLB 5/18/11 07:14 p

LOG OF BORING NO. B-5
Sausal Creek Restoration Project
Oakland, California

APPENDIX B

Borehole Logs for PT-1 and PT-2

Fugro Consultants, Inc.

BOREHOLE LOG

Hole Id: **PT-1**

Project: **NEHRP Piedmont Thrust** Client: **Fugro**

Project No.: **04.79229700** Location: **Co.,Alameda**

Drill Rig:	**CME D-72**	Date Commenced:	**8/17/2015**	Surface Level (ft):		Latitude (°):	
Drilling Type:	**Auger, SPT, Geo Bore**	Date Completed:	**8/17/2015**	Total Drill Depth (ft):	**21**	Longitude (°):	
Drilled by:	**Fine**	Date Backfilled:	**8/17/2015**	Inclination/Bearing:	**90**	No. of Samples:	
Logged by:	**M. Buga**	Checked by:		Depth to Bedrock (ft):	**0**		

Depth, ft (bgl)	Water Graphic	Drill Time (min)	Sample Type	Sample Number	Recovery, %	RQD, %	SPT Record	N-Value	Graphic Log	Material Description	Depth to Contact (ft)	Lab Results: Moisture (%)	Atterberg Limits: LL	Atterberg Limits: PI	Gravel (%)	Sand (%)	Fines (%)	Estimated Field Strength (H7 H6 H5 H4 H3 H2 H1)	Discontinuity Description and Additional Data
0–5				AUGER	100					CLAY, Silty with Gravel; dry; dark yellowish brown; 10-15% subangular sandstone clasts up to 1-2" color change to gray, slightly sandier color change back to dark brown									Hand auger to 5' to clear for utilities using a 6" bucket auger. Geo Barrel from 5'
5–6		3:00		GP	80						6.20								
6–9		4:30		GP	97					CLAY with Sand and Gravel; very dark gray to black; 5-10% fine sand; 5-10% fine gravel up to 0.5"; quartz lithics; roots at contact									Charcoal at 8'
9–11		5:00		GP	0					Clayey SAND; 65-60% sand; 35-40% fines; bottom 0.2' gravelly sand with clay	9.00								No recovery, cuttings are gravelly, similar to bottom of last sample. While cleaning out hole driller encounters resistance, inner barrel was in the hole and tricone bit got stuck in it.
11–13		NA		SPT-1	20														
13–15				SPT-2	40		5 7 8	15											

Notes:

Fugro Consultants, Inc.

BOREHOLE LOG

Hole Id: **PT-1**

Project: **NEHRP Piedmont Thrust** Client: **Fugro**

Project No.: **04.79229700** Location: **Co.,Alameda**

Drill Rig:	**CME D-72**	Date Commenced:	**8/17/2015**	Surface Level (ft):		Latitude (°):	
Drilling Type:	**Auger, SPT, Geo Bore**	Date Completed:	**8/17/2015**	Total Drill Depth (ft):	**21**	Longitude (°):	
Drilled by:	**Fine**	Date Backfilled:	**8/17/2015**	Inclination/Bearing:	**90**	No. of Samples:	
Logged by:	**M. Buga**	Checked by:		Depth to Bedrock (ft):	**0**		

Depth, ft (bgl)	Water Graphic	Drill Time (min)	Sample Type	Sample Number	Recovery, %	RQD, %	SPT Record	N-Value	Graphic Log	Material Description	Depth to Contact (ft)	Lab Results: Moisture (%)	Atterberg Limits: LL	Atterberg Limits: PI	Gravel (%)	Sand (%)	Fines (%)	Estimated Field Strength (H7 H6 H5 H4 H3 H2 H1)	Discontinuity Description and Additional Data
											15.50								Tricone bit to 15.5' for SPT.
16				SPT-3	20		8 10 12	22		GRAVEL with Clay and Sand; yellowish brown; fine to medium gravel; fine sand; 10% fines; trace large gravel in shoe									
17																			
18				SPT-4	87		15 16 17	33		SILTSTONE dark gray, with gravel clasts; appears to be weathered bedrock with clay seams or matrix	18.00								
19																			
20				SPT-5	80		13 18 23	41											
21											21.00								
										Borehole terminated at 21.00 ft									
22																			
23																			
24																			
25																			
26																			
27																			
28																			
29																			
30																			

Notes:

Fugro Consultants, Inc.

BOREHOLE LOG

Hole Id: **PT-2**

Project: **NEHRP Piedmont Thrust** Client: **Fugro**

Project No.: **04.79229700** Location: **Co.,Alameda**

Drill Rig:	**CME D-72**	Date Commenced:	**8/18/2015**	Surface Level (ft):		Latitude (°):	
Drilling Type:	**Auger, SPT, Geo Bore**	Date Completed:	**8/19/2015**	Total Drill Depth (ft):	**82**	Longitude (°):	
Drilled by:	**Fine**	Date Backfilled:	**8/19/2015**	Inclination/Bearing:	**90**	No. of Samples:	
Logged by:	**M. Buga**	Checked by:		Depth to Bedrock (ft):	**0**		

Depth, ft (bgl)	Water Graphic	Drill Time (min)	Sample Type	Sample Number	Recovery, %	RQD, %	SPT Record	N-Value	Graphic Log	Material Description	Depth to Contact (ft)	Lab Results: Moisture (%)	Atterberg Limits: LL	Atterberg Limits: PI	Gravel (%)	Sand (%)	Fines (%)	Estimated Field Strength (H7 H6 H5 H4 H3 H2 H1)	Discontinuity Description and Additional Data
				AUGER	100					Lean CLAY	1.00								Hand auger to 6' to clear utilities
										Sandy SILT with Gravel; dark yellowish brown; 75-80% fines; 15-20% fine to medium sand; 5% fine gravel									
7				SPT-1	93		6 6 6	12											Drillers pull mud tub off previous hole, clean out hole and take SPT-2
8				SPT-2	60		8 7 4	11			8.40								
										CLAY; silty with sand; dark yellowish brown; 90-95% medium to high plasticity fines; 5-10% fine sand; trace gravel									Switch to Geo Barrel at 9'
10		6:00		GP	100														
11																			
12		2:30		GP	100					becomes yellowish brown with greenish gray mottling below 11.2'									
13																			
14		13:00		GP	100														
15																			

Notes:

Fugro Consultants, Inc.

BOREHOLE LOG

Hole Id: **PT-2**

Project: **NEHRP Piedmont Thrust** Client: **Fugro**

Project No.: **04.79229700** Location: **Co.,Alameda**

Drill Rig:	**CME D-72**	Date Commenced:	**8/18/2015**	Surface Level (ft):		Latitude (°):	
Drilling Type:	**Auger, SPT, Geo Bore**	Date Completed:	**8/19/2015**	Total Drill Depth (ft):	**82**	Longitude (°):	
Drilled by:	**Fine**	Date Backfilled:	**8/19/2015**	Inclination/Bearing:	**90**	No. of Samples:	
Logged by:	**M. Buga**	Checked by:		Depth to Bedrock (ft):	**0**		

Depth, ft (bgl)	Water Graphic	Drill Time (min)	Sample Type	Sample Number	Recovery, %	RQD, %	SPT Record	N-Value	Graphic Log	Material Description	Depth to Contact (ft)	Lab Results: Moisture (%)	Atterberg Limits: LL	Atterberg Limits: PI	Gravel (%)	Sand (%)	Fines (%)	Estimated Field Strength (H7 H6 H5 H4 H3 H2 H1)	Discontinuity Description and Additional Data
16										below 15'; becomes sandy and gravelly; 30% sand; 15-20% gravel; gravels consist of sandstone, rare cobble; sandstone gravels are red and heavily weathered								Slow drilling 16-17'
17																			
18																			
19																			
20		14:00		GP	100						19.70								
										Sandy CLAY; moist; reddish yellowish brown; trace gravels; root at 20.3' with reduction; sand is fine to coarse									
21																			
22																			
23										22.9-23.1' becomes gravelly; 20% subangular gravel 0.1-0.5" below 23.1' 10% fine gravel									
24																			
25		9:30		GP	100														
26																			
27											27.00								
28										Sandy CLAY; as above but with thin clay beds, thinnly spaced; 25-30% fine to medium sand; beds are horizontal									
29																			
30		NA		GP	100														

Notes:

Fugro Consultants, Inc.

BOREHOLE LOG

Hole Id: **PT-2**

Project: **NEHRP Piedmont Thrust** Client: **Fugro**

Project No.: **04.79229700** Location: **Co.,Alameda**

Drill Rig:	**CME D-72**	Date Commenced:	**8/18/2015**	Surface Level (ft):		Latitude (°):	
Drilling Type:	**Auger, SPT, Geo Bore**	Date Completed:	**8/19/2015**	Total Drill Depth (ft):	**82**	Longitude (°):	
Drilled by:	**Fine**	Date Backfilled:	**8/19/2015**	Inclination/Bearing:	**90**	No. of Samples:	
Logged by:	**M. Buga**	Checked by:		Depth to Bedrock (ft):	**0**		

Depth, ft (bgl)	Water Graphic	Drill Time (min)	Sample Type	Sample Number	Recovery, %	RQD, %	SPT Record	N-Value	Graphic Log	Material Description	Depth to Contact (ft)	Lab Results: Moisture (%)	Atterberg Limits: LL	Atterberg Limits: PI	Gravel (%)	Sand (%)	Fines (%)	Estimated Field Strength (H7 H6 H5 H4 H3 H2 H1)	Discontinuity Description and Additional Data
31										below 30.5' sandier, 30% sand									
32										31.7-32.4' 15% gravel									
33										32.4-33' gradational color change to bluish gray									
34		9:50		GP	100														
35										34.0-34.2 sand with gravel interbeds 35-35.7 sand with gravel interbeds									
36																			
37										36.5' 15% gravel									Finish for the day at 4:00 pm, pick up site Begin 8/19/2015 at 6:30 am
38										Clayey GRAVEL with Sand; greenish gray; 50% angular to subangular gravels up to 0.5"; 30% sand; 20% fines; chert lithics	37.30								
39										Clayey SAND; light brown; 80-85% fine to coarse sand; 15-20% fines	38.50								
40		8:30		GP	92														
41										40.4-40.6' 25-30% gravel below 40.6' 10-15% gravel and coarse sand									
42																			
43																			
44										43-43.2' sandy gravel 43.6-43.8' sandy gravel 43.8-44.9' horizontally bedded sand									
45		7:45		GP	100														

Notes:

Fugro Consultants, Inc.

BOREHOLE LOG

Hole Id: **PT-2**

Project: **NEHRP Piedmont Thrust** Client: **Fugro**

Project No.: **04.79229700** Location: **Co.,Alameda**

Drill Rig:	**CME D-72**	Date Commenced:	**8/18/2015**	Surface Level (ft):		Latitude (°):	
Drilling Type:	**Auger, SPT, Geo Bore**	Date Completed:	**8/19/2015**	Total Drill Depth (ft):	**82**	Longitude (°):	
Drilled by:	**Fine**	Date Backfilled:	**8/19/2015**	Inclination/Bearing:	**90**	No. of Samples:	
Logged by:	**M. Buga**	Checked by:		Depth to Bedrock (ft):	**0**		

Depth, ft (bgl)	Water Graphic	Drill Time (min)	Sample Type	Sample Number	Recovery, %	RQD, %	SPT Record	N-Value	Graphic Log	Material Description	Depth to Contact (ft)	Lab Results: Moisture (%)	Atterberg Limits: LL	Atterberg Limits: PI	Gravel (%)	Sand (%)	Fines (%)	Estimated Field Strength (H7 H6 H5 H4 H3 H2 H1)	Discontinuity Description and Additional Data
46										44.9-45.4' sandy gravel with clay, well indurated, weathered sandstone gravels below 45.5' interbedded clayey sand with gravel and clay, thinnly bedded									
47																			
48		7:40		GP	50					47-47.5' clayey sand with gravel 47.5-48' clayey gravel 48-48.2' sandy clay 48.2-49.5' clayey sand with gravel; fine to coarse sand; 5-10% gravels appx 0.1-0.4"; 30% clay									
49																			
50																			
51																			
52																			Rig chatter
53		4:00		GP	100					fine to medium sand with 10% clay									
54										53.4' gravelly sand with clay; 20% gravel, rare cobble; sandstone and chert lithics									
55		7:00		GP	73					abundant chert gravels 30-40% with rare cobble									Rig chatter 55-57'
56																			
57																			
58		2:30		GP	70														
59																			
60																			

Notes:

Fugro Consultants, Inc.

BOREHOLE LOG

Hole Id: **PT-2**

Project: **NEHRP Piedmont Thrust** Client: **Fugro**

Project No.: **04.79229700** Location: **Co.,Alameda**

Drill Rig:	**CME D-72**	Date Commenced:	**8/18/2015**	Surface Level (ft):		Latitude (°):	
Drilling Type:	**Auger, SPT, Geo Bore**	Date Completed:	**8/19/2015**	Total Drill Depth (ft):	**82**	Longitude (°):	
Drilled by:	**Fine**	Date Backfilled:	**8/19/2015**	Inclination/Bearing:	**90**	No. of Samples:	
Logged by:	**M. Buga**	Checked by:		Depth to Bedrock (ft):	**0**		

Depth, ft (bgl)	Water Graphic	Drill Time (min)	Sample Type	Sample Number	Recovery, %	RQD, %	SPT Record	N-Value	Graphic Log	Material Description	Depth to Contact (ft)	Lab Results: Moisture (%)	Atterberg Limits: LL	Atterberg Limits: PI	Gravel (%)	Sand (%)	Fines (%)	Estimated Field Strength (H7 H6 H5 H4 H3 H2 H1)	Discontinuity Description and Additional Data
61–62		2:00		GP	100					clayey gravel with sand; yellowish brown; 40% gravel to 61.5', below 61.5' sandy clay with trace gravel 5-10% gravel									
62–65		4:00		GP	123														0.7' recovered in Run 15 from previous runs
65–67		5:30		GP	100					CLAY; brown to olive gray; highly weathered to residual soil; massive; becomes gray below 66.7'	65.40								
67–72		12:00		GP	100					68.8-69' clayey sand interbed 70-70.6' clayey sand									
72–75		9:20		GP	100					0.05-0.1' thick interbeds of sandy clay 74.2-74.8' clayey sand									

Notes:

Fugro Consultants, Inc.

BOREHOLE LOG

Hole Id: **PT-2**

Project: **NEHRP Piedmont Thrust** Client: **Fugro**

Project No.: **04.79229700** Location: **Co.,Alameda**

Drill Rig:	**CME D-72**	Date Commenced:	**8/18/2015**	Surface Level (ft):		Latitude (°):	
Drilling Type:	**Auger, SPT, Geo Bore**	Date Completed:	**8/19/2015**	Total Drill Depth (ft):	**82**	Longitude (°):	
Drilled by:	**Fine**	Date Backfilled:	**8/19/2015**	Inclination/Bearing:	**90**	No. of Samples:	
Logged by:	**M. Buga**	Checked by:		Depth to Bedrock (ft):	**0**		

Depth, ft (bgl)	Water Graphic	Drill Time (min)	Sample Type	Sample Number	Recovery, %	RQD, %	SPT Record	N-Value	Graphic Log	Material Description	Depth to Contact (ft)	Lab Results: Moisture (%)	Atterberg Limits: LL	Atterberg Limits: PI	Gravel (%)	Sand (%)	Fines (%)	Estimated Field Strength (H7 H6 H5 H4 H3 H2 H1)	Discontinuity Description and Additional Data
76										75.1-75.4' clayey sand clayey sand; olive gray; fine to medium sand; massive									
77																			
78																			
79										CLAY; greenish gray; massive	78.70								
		10:00		GP	100					Gravelly lean CLAY; dark reddish brown; increasing gravel and sand content with depth to 81' where it is gravelly sand with clay	79.40								
80																			
81																			
82										Borehole terminated at 82.00 ft	82.00								
83																			
84																			
85																			
86																			
87																			
88																			
89																			
90																			

Notes: